12-1998

Synergistic algorithm for estimating vegetation canopy leaf area index and fraction of absorbed photosynthetically active radiation from MODIS and MISR data

Yuri Knyazikhin

J. V. Martonchik

Ranga B. Myneni

D. J. Diner

Steven W. Running
University of Montana - Missoula

Recommended Citation
Knyazikhin, Y., J. V. Martonchik, R. B. Myneni, D. J. Diner, and S. W. Running (1998), Synergistic algorithm for estimating vegetation canopy leaf area index and fraction of absorbed photosynthetically active radiation from MODIS and MISR data, J. Geophys. Res., 103(D24), 32257–32275, doi:10.1029/98JD02462

JOURNAL OF GEOPHYSICAL RESEARCH, VOL. 103, NO. D24, PAGES 32,257–32,275, DECEMBER 27, 1998

Synergistic algorithm for estimating vegetation canopy leaf area index and fraction of absorbed photosynthetically active radiation from MODIS and MISR data

Y. Knyazikhin,[1] J.V. Martonchik,[2] R.B. Myneni,[1] D.J. Diner,[2] and S. W. Running[3]

Abstract. A synergistic algorithm for producing global leaf area index and fraction of absorbed photosynthetically active radiation fields from canopy reflectance data measured by MODIS (moderate resolution imaging spectroradiometer) and MISR (multiangle imaging spectroradiometer) instruments aboard the EOS-AM 1 platform is described here. The proposed algorithm is based on a three-dimensional formulation of the radiative transfer process in vegetation canopies. It allows the use of information provided by MODIS (single angle and up to 7 shortwave spectral bands) and MISR (nine angles and four shortwave spectral bands) instruments within one algorithm. By accounting features specific to the problem of radiative transfer in plant canopies, powerful techniques developed in reactor theory and atmospheric physics are adapted to split a complicated three-dimensional radiative transfer problem into two independent, simpler subproblems, the solutions of which are stored in the form of a look-up table. The theoretical background required for the design of the synergistic algorithm is discussed.

1. Introduction

Large-scale ecosystem modeling is used to simulate a range of ecological responses to changes in climate and chemical composition of the atmosphere, including changes in the distribution of terrestrial plant communities across the globe in response to climate changes. Leaf area index (LAI) is a state parameter in all models describing the exchange of fluxes of energy, mass (e.g., water and CO_2), and momentum between the surface and the planetary boundary layer. Analyses of global carbon budget indicate a large terrestrial middle- to high-latitude sink, without which the accumulation of carbon in the atmosphere would be higher than the present rate. The problem of accurately evaluating the exchange of carbon between the atmosphere and the terrestrial vegetation therefore requires special attention. In this context the fraction of photosynthetically active radiation (FPAR) absorbed by global vegetation is a key state variable in most ecosystem productivity models and in global models of climate, hydrology, biogeochemestry, and ecology [*Sellers et al.*, 1997]. Therefore these variables that describe vegetation canopy structure and its energy absorption capacity are required by many of the EOS Interdisciplinary Projects [*Myneni et al.*, 1997a]. In order to quantitatively and accurately model global dynamics of these processes, differentiate short-term from long-term trends, as well as to distinguish regional from global phenomena, these two parameters must be collected often for a long period of time and should represent every region of the Earth's lands. Satellite remote sensing serves as the most effective means for collecting global data on a regularly basis. The launch of EOS-AM 1 with MODIS (moderate resolution imaging spectroradiometer) and MISR (multiangle imaging spectroradiometer) instruments onboard begins a new era in remote sensing the Earth system. In contrast to previous single-angle and single-channel instruments, MODIS and MISR together allow for rich spectral and angular sampling of the radiation field reflected by vegetation canopies. This sets new demands on the retrieval techniques for geophysical parameters in order to take full advantages of these instruments. Our objective is to derive a synergistic algorithm for the extraction of LAI and FPAR from MODIS- and MISR-measured canopy reflectance data, with the flexibility to use the same algorithm in MODIS-only and MISR-only as well. Although a prototyping of the algorithm with data was also a focus of our activity, these results are not discussed in this article. Plate 1 demonstrates an example of the prototype of the MODIS LAI/FPAR data product.

Solar radiation scattered from a vegetation canopy and measured by satellite sensors results from interaction of photons traversing through the foliage medium, bounded at the bottom by a radiatively participating surface. Therefore to estimate the canopy radiation regime, three important features must be carefully formulated. They are (1) the architecture of individual plant and the entire canopy; (2) optical properties of vegetation elements (leaves, stems) and soil; the former depends on physiological conditions (water status, pigment concentration); and (3) atmospheric conditions which determine the incident radiation field. Photon transport theory aims at deriving the solar radiation regime, both within the

[1]Department of Geography, Boston University, Massachusetts.
[2]Jet Propulsion Laboratory, California Institute of Technology.
[3]The School of Forestry, University of Montana, Missoula.

Paper number 98JD02462.
0148-0227/98/98JD-02462$09.00

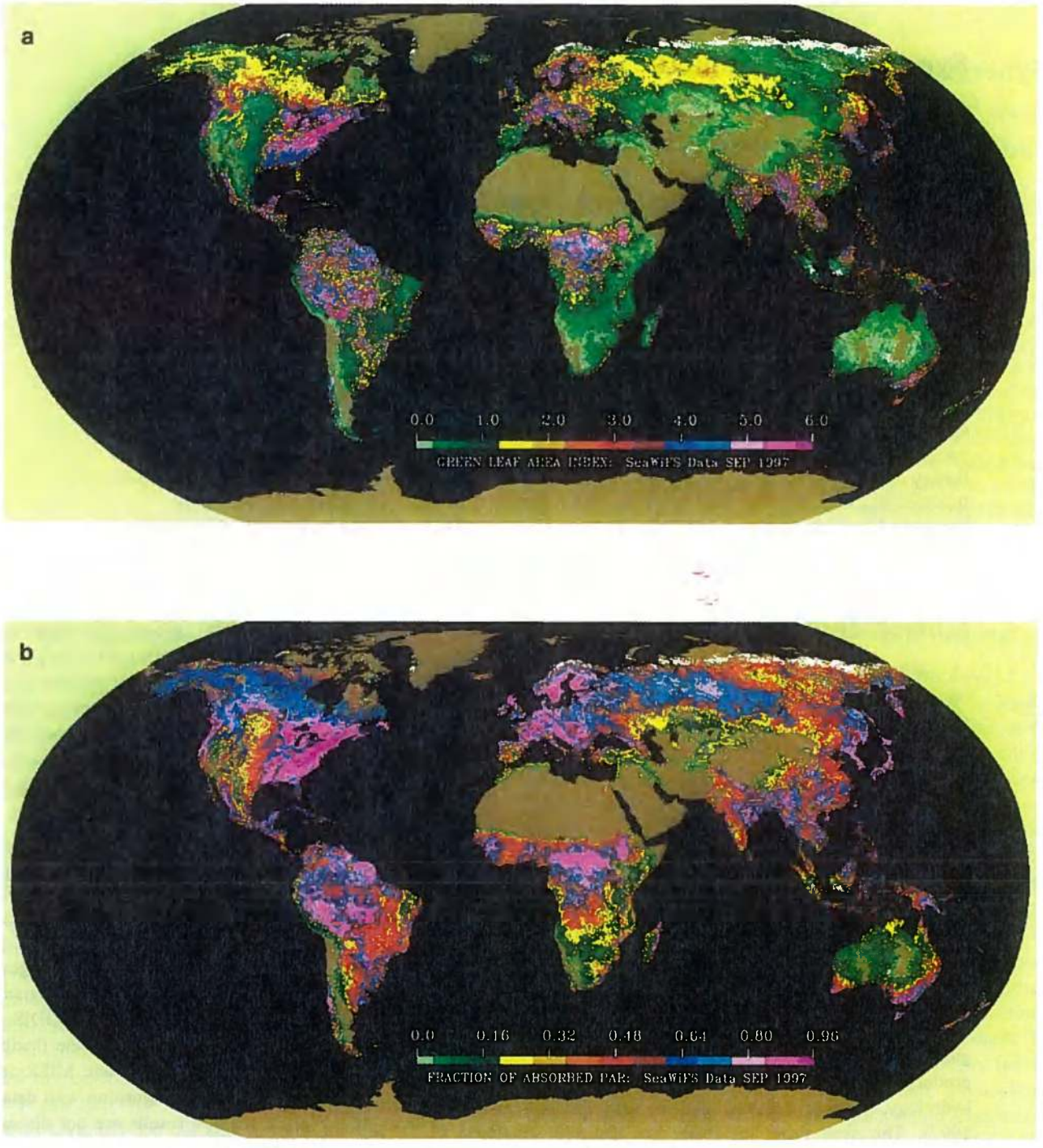

Plate 1. (a) Global LAI and (b) FPAR in September-October 1997 derived from SeaWiFs (sea-viewing wide field-of-view sensor) data. This data set includes daily atmosphere-corrected surface reflectances at eight shortwave spectral bands. Surface reflectances at red (670 nm) and near-infrared (865 nm) at 8 km resolution were used. The algorithm was applied to daily surface reflectance data for all days from September 18 to October 12, 1997. For each pixel, LAI and FPAR values corresponding to the maximum NDVI during this period are shown in these pannels. The look-up table for biome 1 (grasses and cereal crops, Table 1) was used to produce global LAI and FPAR for all biome types.

vegetation canopy and the radiant exitance, using the above mentioned attributes as input data. This theory underlies numerous canopy radiation models (see, for example, reviews by *Myneni et al.* [1989] and *Ross et al.* [1992]). Usually retrieval techniques rely on a model, which provide relationships between measured data and biophysical parameters. It allows for the design of fast retrieval algorithms. However, such algorithms can retrieve only those variables that are explicitly represented in the canopy radiation models. They exclude the use of a rather wide family of three-dimensional models in which desired variables may not be in the model parameter list directly [*Ross and Marshak*, 1984; *Myneni*, 1991; *Borel et al.*, 1991; *Kimes*, 1991; *Knyazikhin et al.*, 1996]. They are also based on some assumptions which may not be fulfilled. For example, numerous canopy radiation models presuppose that the canopy angular reflectance measurements can be performed about the plane of the solar vertical which provides information on the hot spot effect [*Kuusk*, 1985; *Simmer and Gerstl*, 1985; *Marshak*, 1989; *Verstraete et al.*, 1990; *Myneni et al.*, 1991]. This suggestion may be appropriate for multiangle instruments such as MISR or POLDER (Polarization and Directionality of the Earth's Reflectance) [*Deschamps et al.*, 1994]. For the single-angle and multichannel MODIS instrument, this suggestion is not fulfilled. There is yet another problem encountered when one incorporates a particular model in the inverse mode. A rather wide family of canopy radiation models designed to account for the hot spot effect conflict with the law of energy conservation (Appendix); that is, they are not "physically based" models.

In designing the synergistic algorithm, we cast aside the idea of trying to relate a retrieval technique with a particular canopy radiation model. Our approach incorporates the following tenets: (1) a retrieval algorithm can use any field-tested canopy radiation model; that is, the retrieval algorithm is model independent; (2) the more measured information is available and the more accurate this information is, the more reliable and accurate the algorithm output would be, i.e., convergence of the algorithm; (3) the algorithm must be as simple as the one linked to a particular canopy radiation model; (4) spectral and angular information are synergistically used in the extraction of LAI and FPAR. Because three-dimensional models include all diversity of one- and two-dimensional models as special cases, property (1) of the algorithm can be achieved, if one formulates the inverse problem for three-dimensional vegetation canopies: given mean spectral, and in the case of MISR data, angular signatures of canopy-leaving radiance averaged over the three-dimensional canopy radiation field, find LAI and FPAR. It is clear that the given information is not enough to solve the inverse problem. For example, the three-dimensional canopy structure can vary considerably with LAI essentially unchanged. Therefore one needs to limit the range of variation of the variables determining the three-dimensional radiative regime in plant canopies. It can be achieved by using a vegetation cover classification parameterized in terms of variables used by photon transport theory [*Myneni et al.*, 1997]. It distinguishes six biome types, each representing a pattern of the architecture of an individual tree (leaf normal orientation, stem-trunk-branch area fractions, leaf and crown size) and the entire canopy (trunk distribution, topography), as well as patterns of spectral reflectance and transmittance of vegetation elements. The soil and/or understory type are also characteristics of the biome, which can vary continuously within given biome-dependent ranges. The distribution of leaves is described by the leaf area density distribution function which also depends on some continuous parameters. A detailed description of biome types is presented in section 2.

The canopy structure is the most important variable determining the three-dimensional radiation field in vegetation canopies. Therefore section 3 starts with a precise mathematical definition of this variable and how various canopy radiation models treat this variable. This allows us to specify some common properties of the present canopy radiation models. The basic physical principle underlying the proposed LAI/FPAR retrieval algorithm is the law of energy conservation. However, a rather wide family of canopy radiation models (described in the Appendix) conflict with this law. Therefore the three-dimensional transport equation which includes a nonphysical internal source is taken as the starting point for the derivation of the algorithm. In section 4, a technique developed in atmospheric optics is utilized to parameterize the radiative field in terms of reflectance properties of the canopy and ground, as well as to split the radiative transfer problem into two independent subproblems, each of which is expressed in terms of three basic components of the energy conservation law: canopy transmittance, reflectance, and absorptance. These components are elements of the look-up table (LUT), and the algorithm interacts only with the elements of the LUT. This provides the required independence of the retrieval algorithm to a particular canopy radiation model. The next important step in achieving property (3) is to specify the dependence of canopy transmittance, reflectance, and absorptance on wavelength. It is precisely derived in section 5; this dependence is described by a simple function which depends on the unique positive eigenvalue of the transport equation. The eigenvalue relates optical properties of individual leaves to canopy structure. This result not only allows a significant reduction in the size of the LUT but also relates canopy spectral reflectance with spectral properties of individual leaves, which is a rather stable characteristic of green leaves.

In spite of the essential reduction of possible canopy representatives by introducing a vegetation cover classification, the inverse problem still allows for multiple solutions. A technique allowing the reduction of nonphysical solutions is described in section 6. A definition of the LUT is given in this section as well. A method to estimate the most probable LAI and FPAR, accounting for specific features of the MODIS and MISR instruments, and providing convergence of the algorithm is discussed in sections 7 and 8. The maximum positive eigenvalue and the unique positive eigenvector corresponding to this eigenvalue, detailed in section 5, express the law of energy conservation in a compact form. The results of this section allow us to relate the

Normalized Difference Vegetation Index (NDVI) to this fundamental physical principle. Relationships between FPAR and NDVI are also used in our algorithm as a backup to the LUT approach, and so we discuss these in section 9.

2. Canopy Structural Types of Global Vegetation

Solar radiation scattered from a vegetation canopy and measured by satellite sensors results from interaction of photons traversing through the foliage medium, bounded at the bottom by a radiatively participating surface. Therefore to estimate the canopy radiation regime, three important features must be carefully formulated [*Ross*, 1981]. They are (1) the architecture of individual plants or trees and the entire canopy; (2) optical properties of vegetation elements (leaves, stems) and ground; the former depends on physiological conditions (water status, pigment concentration); and (3) atmospheric conditions which determine the incident radiation field. Photon transport theory aims at deriving the solar radiation regime, both within the vegetation canopy and radiant exitance, using the above mentioned attributes as input data. This underlies a land cover classification [*Myneni et al.*, 1997] which is compatible with the basic physical principle of transport theory, the law of energy conservation. Global land covers can be classified into six types (biomes), depending on their canopy structure (Table 1). The structural attributes of these land covers can be parameterized in terms of variables that transport theory admits as follows.

The heterogeneity of the plant canopy can be described by the three-dimensional leaf area distribution function u_L. Its values at spatial points depend on trunk distribution, topography, stem-trunk-branch area fraction, foliage dispersion, leaf and crown size, and leaf clumping [*Myneni and Asrar*, 1991; *Oker-Blom et al.*, 1991]. The three-dimensional distribution of leaves determines various models to account for shadowing effects [*Kuusk*, 1985; *Li and Strahler*, 1985; *Verstraete et al.*, 1990].

The leaf area index LAI is defined as

$$\mathrm{LAI} = \frac{1}{X_S \cdot Y_S} \int_V u_L(r)\, dr\,, \qquad (1)$$

where V is the domain in which a plant canopy is located; X_S, Y_S are horizontal dimensions of V. If the vegetation canopy consists of N_c individual trees, LAI can be expressed as

$$\mathrm{LAI} = \sum_{k=1}^{N_C} p_k \frac{1}{S_k} \int_{V_k} u_L(r)\, dr = \sum_{k=1}^{N_C} p_k \cdot \mathrm{LAI}_k\,,$$

where S_k is the foliage envelope projection (e.g., crown) of the kth plant or tree onto the ground; $p_k = S_k/(X_S \cdot Y_S)$ and LAI_k is the leaf area index of an individual plant or tree. Thus LAI is

$$\mathrm{LAI} = g \cdot \mathrm{LAI}_0\,,$$

where $g = \sum_{k=1}^{N_C} p_k$ is the ground cover and

$$\mathrm{LAI}_0 = \frac{1}{g} \sum_{k=1}^{N_C} p_k \cdot \mathrm{LAI}_k$$

is the mean LAI of a single plant or tree. The spatial distribution of plants or trees in the stand is a characteristic of the biome type and is assumed known. For each biome type, the leaf area density distribution function is parameterized in terms of ground cover and mean leaf area index of an individual plant or tree, each varying within given biome specific intervals $[g_{\min}, g_{\max}]$ and $[L_{\min}, L_{\max}]$, respectively. Thus the vegetation canopy is represented as a domain V consisting of identical plants or trees in order to numerically evaluate the transport equation.

To parameterize the contribution of the surface underneath the canopy (soil and/or understory) to the canopy radiation regime, an effective ground reflectance is introduced, namely,

$$\rho_{q,\mathrm{eff}}(\lambda) = \frac{\int_{2\pi-}\int_{2\pi+} R_{b,\lambda}(\Omega',\Omega)|\mu\mu'|L_\lambda(r_b,\Omega')\,d\Omega d\Omega'}{\pi \int_{2\pi-} q(\Omega')|\mu'|L_\lambda(r_b,\Omega')\,d\Omega'}. \qquad (2)$$

Here L_λ is radiance at a point r_b of the canopy bottom; $R_{b,\lambda}$ is the bidirectional reflectance factor of the canopy bottom. The function q is a wavelength-independent configurable function

Table 1. Canopy Structural Attributes of Global Land Covers From the Viewpoint of Radiative Transfer Modeling

	Grasses and Cereal Crops	Shrubs	Broadleaf Crops	Savannas	Broadleaf Forests	Needle Forests
Horizontal heterogeneity	no	yes	variable	yes	yes	yes
Ground cover	100%	20-60%	10-100%	20-40%	> 70%	> 70%
Vertical heterogeneity (leaf optics and LAD)	no	no	no	yes	yes	yes
Stems/trunks	no	no	green stems	yes	yes	yes
Understory	no	no	no	grasses	yes	yes
Foliage dispersion	minimal clumping	random	regular	minimal clumping	clumped	severe clumping
Crown shadowing	no	not mutual	no	no	yes mutual	yes mutual
Brightness of canopy ground	medium	bright	dark	medium	dark	dark

used to better account for specific features of various biomes, and it satisfies the following condition:

$$\int_{2\pi-} q(\Omega')d\Omega' = 1. \quad (3)$$

Note that the effective ground reflectance depends on the radiation regime in the vegetation canopy. It follows from the definition that the variation of $\rho_{q,\text{eff}}$ satisfies the following inequality:

$$\min_{\Omega'\in 2\pi-} \frac{\int_{2\pi+} R_{b,\lambda}(\Omega',\Omega)|\mu|d\Omega}{\pi\, q(\Omega')} \le \rho_{q,\text{eff}}(r_b,\lambda) \le \max_{\Omega'\in 2\pi-} \frac{\int_{2\pi+} R_{b,\lambda}(\Omega',\Omega)|\mu|d\Omega}{\pi\, q(\Omega')}; \quad (4)$$

that is, the range of variations depends on the integrated bidirectional factor of the ground surface only. The bidirectional reflectance factor of the ground surface $R_{b,\lambda}$ and the effective ground reflectance are assumed to be horizontally homogeneous; that is, they do not depend on the spatial point r_b. The pattern of the effective ground reflectances (ρ_1, ρ_2, ..., ρ_{11}), $\rho_i=\rho_{q,\text{eff}}(\lambda_i)$, at the MODIS and MISR spectral bands (Table 2), is taken as a parameter characterizing hemispherically integrated reflectance of the canopy ground (soil and/or understory) and can vary continuously within the interval defined by equation (4). The lower and upper bounds of equation (4) depend on biome type. The set of various patterns of effective ground reflectances is a static table of the algorithm, i.e., element of the look-up table. The present version of the look-up table contains 25 patterns of effective ground reflectances evaluated from the soil reflectance model of *Jacquemoud et al.* [1992], using model inputs presented by *Baret et al.* [1993]. Figure 1 demonstrates spectral ground reflectances $\rho_{q,\text{eff}}$ for biome 1 (grasses and cereal crops).

To account for the anisotropy of the ground surface, an effective ground anisotropy S_q is used,

Table 2. MODIS and MISR Spectral Bands

Bands	Center of Spectral Band, nm	Instrument
1	648	MODIS
2	858	MODIS
3	470	MODIS
4	555	MODIS
5	1240	MODIS
6	1640	MODIS
7	2130	MODIS
1	446	MISR
2	558	MISR
3	672	MISR
4	866	MISR

$$S_q(r_b,\Omega) = \frac{1}{\rho_{q,\text{eff}}(\lambda)} \frac{\int_{2\pi-} R_{b,\lambda}(\Omega',\Omega)|\mu'|L_\lambda(r_b,\Omega')d\Omega'}{\pi \int_{2\pi-} q(\Omega')|\mu'|L_\lambda(r_b,\Omega')d\Omega'}, \quad (5)$$

$$r_b \in \delta V_b, \qquad \Omega \bullet n_b < 0,$$

where n_b is the outward normal at point r_b. The effective ground anisotropy S_q depends on the canopy structure as well as the incoming radiation field. We note the following property:

$$\int_{2\pi+} S_q(r_b,\Omega)|\mu|d\Omega = 1,$$

that is, the integral depends neither on spatial nor on spectral variables. For each biome type, the effective ground anisotropy is assumed wavelength independent. The six cover types presented in Table 1 can now be expressed in terms of the above introduced variables.

2.1. Biome 1, Grasses and Cereal Crops

Canopies exhibit vertical and lateral homogeneity, vegetation ground cover of about 1.0 ($g_{\min}=g_{\max}=1$), plant height generally about a meter or less, erect leaf inclination, no woody material, minimal leaf clumping, and soils of intermediate brightness. The one-dimensional radiative transfer model is invoked in this situation. Leaf clumping is implemented by modifying the projection areas with a clumping factor generally less than 1. The soil reflection is assumed Lambertian; that is, $R_{b,\lambda}=R_{\text{lam},\lambda}$. We also set $q=1$. The effective soil reflection and anisotropy then have the simplified form

$$\rho_{q,\text{eff}}(\lambda)=R_{\text{lam},\lambda}, \qquad S_q(r_b,\Omega)=1/\pi. \quad (6)$$

2.2. Biome 2, Shrubs

Canopies exhibit lateral heterogeneity, low ($g_{\min}=0.2$) to intermediate ($g_{\min}=0.6$) vegetation ground cover, small leaves, woody material, and bright backgrounds. The full three-dimensional (3-D) model is invoked. Hot spot, i.e., enhanced brightness about the retrosolar direction due to absence of shadows [*Privette et al.*, 1994], is modeled by shadows cast on the ground (no mutual shadowing because ground cover is low). This land cover is typical of semiarid regions with extreme hot (brush) or cold (tundra/taiga) temperature regimes and poor soils. For this biome we represent the bidirectional soil reflectance factor $R_{b,\lambda}$ as

$$R_{b,\lambda}(\Omega',\Omega) = R_{1,\lambda}(\Omega')\cdot R_{2,\lambda}(\Omega,\Omega_0), \quad (7)$$

where Ω_0 is the direction of the direct solar radiance. We set

$$q(\Omega') = R_{1,\lambda}(\Omega')/\rho^*_{1,\lambda}. \quad (8)$$

The effective soil reflection and soil anisotropy then have the form

$$\rho_{q,\text{eff}}(\lambda) = \rho^*_{1,\lambda}\,\rho^*_{2,\lambda}(\Omega_0), \quad S_q(r_b,\Omega) = \frac{R_{2,\lambda}(\Omega,\Omega_0)}{\pi\,\rho^*_{2,\lambda}(\Omega_0)}, \quad (9)$$

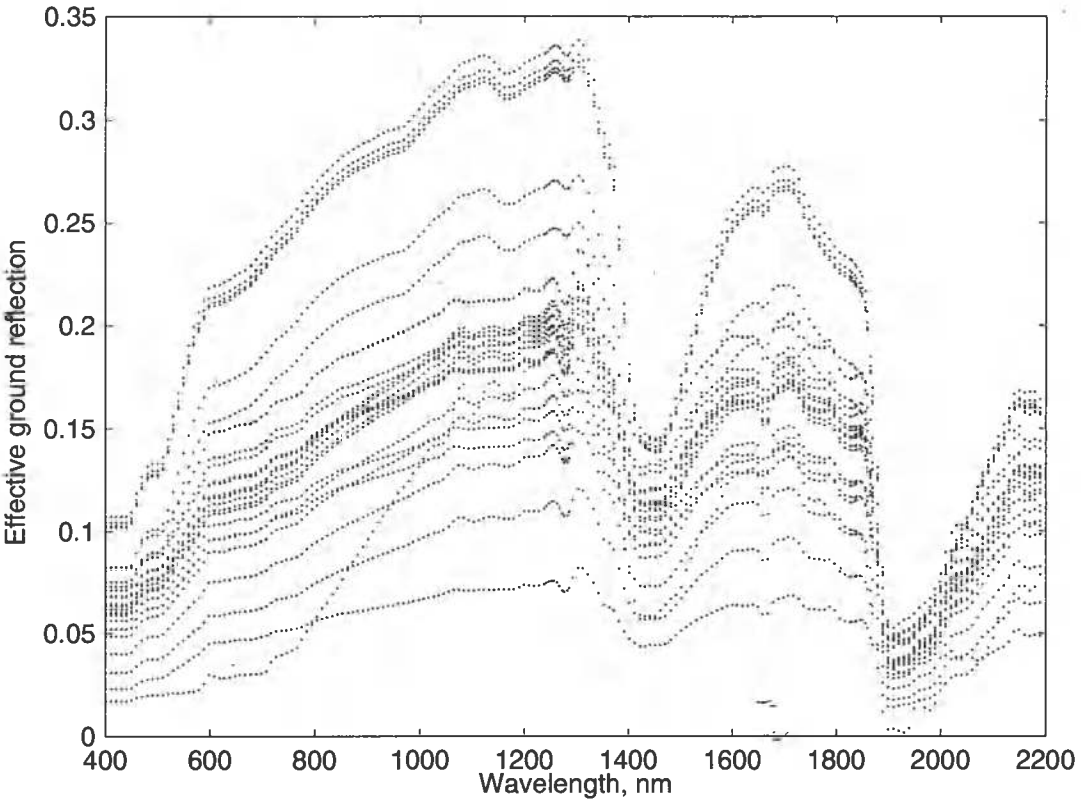

Figure 1. Spectral effective ground reflectance for 25 different soils. It includes three soil types described as mixtures of clay, sand, and peat. Each soil type is characterized by three moisture levels (wet, median, dry) and from two to three soil roughnesses (rough, median, smooth, or rough and smooth). These effective ground reflectances were evaluated from the soil reflectance model of *Jacquemoud et al.* [1992] using model inputs presented by *Baret et al.* [1993].

where

$$\rho^*_{1,\lambda} = \frac{1}{\pi} \int_{2\pi^-} R_{1,\lambda}(\Omega')|\mu'|d\Omega',$$

$$\rho^*_{2,\lambda}(\Omega_0) = \frac{1}{\pi} \int_{2\pi^+} R_{2,\lambda}(\Omega, \Omega_0)|\mu|d\Omega.$$

The functions q and S_q are assumed wavelength independent and serve as parameter of this biome. This biome is characterized by intermediate vegetation ground cover. The use of the above model for the bidirectional soil reflectance factor means that only the incoming direct beam of solar radiation which reaches the soil can influence the anisotropy of the radiation field in the plant canopy.

2.3. Biome 3, Broadleaf Crops

Canopies exhibit lateral heterogeneity, large variations in vegetation ground cover from crop planting to maturity (g_{min}=0.1, g_{max}=1.0), regular leaf spatial dispersion, photosynthetically active, i.e., green, stems, and dark soil backgrounds. The regular dispersion of leaves (i.e., the positive binomial model) leads to a clumping factor that is generally greater than unity. The green stems are modeled as erect reflecting protrusions with zero transmittance. The three-dimensional radiative transfer model is invoked in this situation. The soil reflection is assumed Lambertian, i.e., $R_{b,\lambda}$=$R_{lam,\lambda}$. The function q=1. The effective soil reflection and anisotropy are expressed by equation (6).

2.4. Biome 4, Savanna

Canopies with two distinct vertical layers, understory of grass, low ground cover of overstory trees (g_{min}=0.2, g_{max}=0.4), canopy optics, and structure are therefore vertically heterogeneous. The full 3-D method is required. The interaction coefficients have a strong vertical dependency. Savannas in the tropical and subtropical regions are characterized as mixtures of warm grasses and broadleaf trees. In the cooler regimes of the higher latitudes, they are described as mixtures of cool grass and needle trees. The effective soil reflection and soil anisotropy then are simulated by equation (9).

2.5. Biome 5: Broadleaf Forests

Vertical and lateral heterogeneity, high ground cover (g_{min}=0.8, g_{max}=1.0), green understory, mutual shadowing of crowns, foliage clumping, trunks, and branches are included, so the canopy structure and optical properties differ spatially. Mutual shadowing of crowns is handled by modifying the hot spot formulation. Therefore stand density and crown size define this gap parameter. The branches are randomly

oriented, but tree trunks are modeled as erect structures. Both trunk and branch reflectance are specified from measurements. For this biome the three-dimensional transport equation is utilized to evaluate the effective soil reflection and anisotropy as a function of LAI and Sun position. These are intermediate calculations and are used to precompute parameters stored in the LUT.

2.6. Biome 6: Needle Forests

These are canopies with needles, needle clumping on shoots, severe shoot clumping in whorls, dark vertical trunks, sparse green understory, and crown mutual shadowing. This is the most complex case, invoking the full 3-D method with all its options. A typical shoot is modeled to handle needle clumping on the shoots. The shoots are then assumed to be clumped in the crown space. Mutual shadowing by crowns is handled by modifying the hot spot formulation. The branches are randomly oriented but the dark tree trunks are modeled as erect structures. Both trunk and branch reflectance are specified from measurements. The effective soil reflection and anisotropy are evaluated the same way as for biome 5.

3. Radiative Transfer Problem for Vegetation Media

The domain V in which a vegetation canopy is located, is a parallelepiped of horizontal dimensions X_S, Y_S, and biome-dependent height Z_S. The top δV_t, bottom δV_b, and lateral δV_l surfaces of the parallelepiped form the canopy boundary $\delta V=\delta V_t+\delta V_b+\delta V_l$. The structure of the vegetation canopy is defined by an indicator function $\chi(r)$ whose value is 1, if there is a phytoelement at the spatial point r, and zero otherwise. Here the position vector r denotes the Cartesian triplet (x,y,z) with $(0<x<X_S)$, $(0<y<Y_S)$, and $(0<z<Z_S)$, with its origin $O=(0,0,0)$ at the top of the canopy. The indicator function is treated as a random variable. Its distribution function, in the general case, depends on both macroscale (e.g., random dimension of the trees and their spatial distribution) and microscale (e.g., structural organization of an individual tree) properties of the vegetation canopy and includes all three of its components, absolutely continuous, discrete, and singular [*Knyazikhin et al.*, 1998]. In order to approximate this function, a fine spatial mesh is introduced by dividing the domain V into N_ε nonoverlapping fine cells, e_i, $i=1,2,\ldots,N_\varepsilon$, of size $\Delta x=\Delta y=\Delta z$. Each realization $\chi(r)$ of the canopy structure is replaced by its mean over the fine cell e_i as

$$u_L(r)=\frac{1}{m(e_i)}\int_{e_i}\chi(r)\,m(dr),\quad r\in e_i. \tag{10}$$

Here m is a measure suitable to perform the integration of equation (10). The function u_L is the leaf area density distribution function. In the general case, (10) is the Lebesgue integral and it may not coincide with an integral in the "true sense." This integration technique provides the convergence process $u_L\to\chi/m(V)$ when $\varepsilon\to 0$ [*Knyazikhin et al.*, 1998], and so equation (10) can be taken as an approximation of the structure of the vegetation canopy. The accuracy of this approximation depends on size ε of the fine cell e_i. To our knowledge, all existing canopy radiation models are based on the approximation of (10) by a piece-wise continuous function, e.g., describing both the spatial distribution of various geometrical objects like cones, ellipsoids, etc., and the variation of leaf area within a geometrical figure [*Ross and Nilson*, 1968; *Nilson*, 1977; *Ross* 1981; *Norman and Wells*, 1983; *Li et al.*, 1995]. Therefore we proceed with the suggestion that u_L is the random value whose distribution function is described by a piece-wise continuous function. For each realization, the radiation field in such a medium can be expressed as

$$\Omega\bullet\nabla L_\lambda(r,\Omega)+G(r,\Omega)u_L(r)L_\lambda(r,\Omega)=\frac{u_L(r)}{\pi}\int_{4\pi}\Gamma_\lambda(r,\Omega'\to\Omega)L_\lambda(r,\Omega')d\Omega'. \tag{11}$$

Here $\Omega\bullet\nabla$ is the derivative at r along the direction Ω; L_λ is the monochromatic radiance at point r and in the direction Ω,

$$G(r,\Omega)=\frac{1}{2\pi}\int_{2\pi^+}g_L(r,\Omega_L)|\Omega\bullet\Omega_L|d\Omega_L,$$

is the mean projection of leaf normals at r onto a plane perpendicular to the direction Ω; g_L is the probability density of leaf normal distribution over the upper hemisphere $2\pi^+$;

$$\frac{1}{\pi}\Gamma_\lambda(r,\Omega'\to\Omega)=\frac{1}{2\pi}\int_{2\pi^+}g_L(r,\Omega_L)|\Omega'\bullet\Omega_L|\gamma_{L,\lambda}(r,\Omega_L,\Omega'\to\Omega)d\Omega_L,$$

is the area-scattering phase function [*Ross*, 1981], and $\gamma_{L,\lambda}$ is the leaf-scattering phase function. Unit vectors are expressed in spherical coordinates with respect to $(-Z)$ axis. It follows from the above definitions that the solution of the transport equation is also a random variable. For each biome type, the angular distribution of radiance leaving the top surface of the vegetation canopy is defined to be the mean value, $\langle L_\lambda\rangle_{bio}$, of L_λ over different realizations of the given biome type. The following definitions of biome-specific reflectances are used in this paper.

The hemispherical-directional reflectance factor (HDRF) for nonisotropic incident radiation is the ratio of the mean radiance leaving the top of the plant canopy, $\langle L_\lambda(r_t,\Omega)\rangle_{bio}$, $\Omega\bullet n_t>0$, to radiance reflected from an ideal Lambertian target into the same beam geometry and illuminated under identical atmospheric conditions [*Diner et al.*, 1998a]; that is,

$$r_\lambda(\Omega,\Omega_0)=\frac{\langle L_\lambda(r_t,\Omega)\rangle_{bio}}{\frac{1}{\pi}\int_{2\pi^-}L_\lambda(r_t,\Omega')|\Omega'\bullet n_t|d\Omega'},\quad \Omega\bullet n_t>0.$$

Here n_t is the outward normal at points $r_t\in\delta V_t$; $\langle\cdot\rangle_{bio}$ denotes the averaging over the ensemble of biome realizations; and Ω_0 is the direction of the monodirectional solar radiation incident on the top of the canopy boundary.

The bihemispherical reflectance (BHR) for nonisotropic incident radiation is the ratio of the mean radiant exitance to the incident radiant [*Diner et al.*, 1998a], i.e.,

$$A_\lambda^{\text{hem}}(\Omega_0) = \frac{\int_{2\pi+} < L_\lambda(r_t,\Omega) >_{\text{bio}} |\Omega \bullet n_t| d\Omega}{\int_{2\pi-} L_\lambda(r_t,\Omega') |\Omega' \bullet n_t| d\Omega'}.$$

In order to quantify a proportion between direct and diffuse component of incoming radiation, the ratio $f_{\text{dir}}(\Omega_0)$ of direct radiant incident on the top of the plant canopy to the total incident irradiance is used. If $f_{\text{dir}}=1$, HDRF and BHR become the bidirectional reflectance factor (BRF), and the directional hemispherical reflectance (DHR). Here $r_\lambda(\Omega,\Omega_0)$ and $A_\lambda^{\text{hem}}(\Omega_0)$ denote, depending on the situation ($f_{\text{dir}}=1$ or $f_{\text{dir}}\neq 1$), HDRF and BHR or BRF and DHR.

In spite of the diversity of canopy reflectance models, they can be classified with respect to how the averaging over the ensemble of canopy realizations is performed. In terms of equation (11), this is equivalent to how the averaging of $u_L(r)L_\lambda(r,\Omega)$ is performed. In the turbid medium models, the vegetation canopy is treated as a gas with nondimensional planar scattering centers [*Ross*, 1981]. Such models presuppose that

$$\langle u_L(r) L_\lambda(r,\Omega) \rangle_{\text{bio}} = \langle u_L(r) \rangle_{\text{bio}} \langle L_\lambda(r,\Omega) \rangle_{\text{bio}} . \quad (12)$$

As a result, equation (10) is reduced to the classical transport equation [*Ross*, 1981] whose solution is the mean radiance $<L_\lambda(r,\Omega)>_{\text{bio}}$. This technique allows the design of conservative radiation transfer models, i.e., models in which the law of energy conservation holds true for any elementary volume. Such an approach cannot account for the hot spot phenomena because it ignores shadowing effects. This motivated the development of a family of radiative transfer models based on the following fact: the two events that a point inside a leaf canopy can be viewed from two points r_1 and r_2 are not independent [*Kuusk*, 1985]. The mean of $u_L(r)L_\lambda(r,\Omega)$ is presented as

$$\langle u_L(r) L_\lambda(r,\Omega) \rangle_{\text{bio}} = p(r,\Omega,\Omega') \cdot \langle u_L(r) \rangle_{bio} \langle L_\lambda(r,\Omega) \rangle_{\text{bio}} ,$$

where p is the bidirectional gap probability [*Kuusk*, 1985; *Li and Strahler*, 1985; *Verstraete et al.*, 1990; *Oker-Blom et al.*, 1991]. Such models account accurately for once scattered radiance, taking $Gp<u_L>$ as the extinction coefficient. For evaluation of the multiply scattered radiance, assumption (12) is usually used [*Marshak*, 1989; *Myneni et al.*, 1995b]. These types of canopy-radiation models can well simulate BRFs. However, they are not conservative (Appendix 1). The problem of obtaining a correct closed equation for the mean monochromatic radiance was formulated and solved by *Vainikko* [1973], where the equations for the mean radiance were derived through spatial averaging of the stochastic transport equation (11) in a model of broken clouds. This approach was studied in detail by *Titov* [1990]. *Anisimov and Menzulin* [1981] utilized similar ideas to describe the radiation regime in plant canopies. The stochastic models incorporate the best features of the above mentioned approaches. The aim of this paper is to derive some general properties of radiation transfer which do not depend on a particular model and which can be taken as the basis of our LAI/FPAR retrieval algorithm. Equation (11) express the law of energy conservation in the most general form. Therefore our aim can be achieved, if this equation is taken as a starting point for deriving the desired properties. In order to include canopy reflectance models with hot spot effect into consideration, a transport equation of the form

$$\Omega \bullet \nabla L_\lambda(r,\Omega) + G(r,\Omega) u_L(r) L_\lambda(r,\Omega) = \frac{u_L(r)}{\pi} \int_{4\pi} \Gamma_\lambda(r,\Omega' \to \Omega) L_\lambda(r,\Omega') d\Omega' + F_\lambda(r,\Omega) \quad (13)$$

will also be considered in this paper. Here F_λ is a function which accounts for the hot spot effect (Appendix).

Equation (13) alone does not provide a full description of random realizations of the radiative field. It is necessary to specify the incident radiance at the canopy boundary δV i.e., specification of the boundary conditions. Because the canopy is adjacent to the atmosphere, and neighboring canopies, and the soil or understory, all which have different reflection properties, the following boundary conditions will be used to describe the incoming radiation [*Ross et al.*, 1992]:

$$L_\lambda(r_t,\Omega) = L^{\text{top}}_{d,\lambda}(r_t,\Omega,\Omega_0) + L^{\text{top}}_{m,\lambda}(r_t)\delta(\Omega-\Omega_0), \quad (14)$$

$$r_t \in \delta V_t, \qquad \Omega \bullet n_t < 0,$$

$$L_\lambda(r_l,\Omega) = \frac{1}{\pi} \int_{\Omega' \bullet n_l > 0} R_{l,\lambda}(\Omega',\Omega) L_\lambda(r_l,\Omega') |\Omega' \bullet n_l| d\Omega' + L^{\text{lat}}_{d,\lambda}(r_l,\Omega,\Omega_0) + L^{\text{lat}}_{m,\lambda}(r_l)\delta(\Omega-\Omega_0), \quad (15)$$

$$r_l \in \delta V_l, \qquad \Omega \bullet n_l < 0,$$

$$L_\lambda(r_b,\Omega) = \frac{1}{\pi} \int_{\Omega' \bullet n_b > 0} R_{b,\lambda}(\Omega',\Omega) L_\lambda(r_b,\Omega') |\Omega' \bullet n_b| d\Omega', \quad (16)$$

$$r_b \in \delta V_b, \qquad \Omega \bullet n_b < 0,$$

where $L^{\text{top}}{}_{d,\lambda}$ and $L^{\text{top}}{}_{m,\lambda}$ are the diffuse and monodirectional components of solar radiation incident on the top surface of the canopy boundary δV_t; $\Omega_0 \sim (\mu_0,\phi_0)$ is the direction of the monodirectional solar component; δ is the Dirac delta function; $L^{\text{lat}}{}_{m,\lambda}$ is the intensity of the monodirectional solar radiation arriving at a point $r_l \in \delta V_l$ along Ω_0 without experiencing an interaction with the neighboring canopies; $L^{\text{lat}}{}_{d,\lambda}$ is the diffuse radiation penetrating through the lateral surface δV_l; $R_{L\lambda}$ and $R_{b,\lambda}$ (in sr^{-1}) are the bidirectional reflectance factors of the lateral and the bottom surfaces, respectively; and n_t, n_l, and n_b are the outward normals at points $r_t \in \delta V_t$, $r_l \in \delta V_l$ and $r_b \in \delta V_b$, respectively. A solution of the boundary value problem, expressed by equations (13)-(16), describes a random realization of the radiation field in a vegetation canopy.

4. Mathematical Basis of the Algorithm

The aim of this section is to parameterize the contribution of soil/understory reflectances to the exitant radiation field. We closely follow ideas used in atmospheric physics [*Kondratyev*, 1969; *Liou*, 1980]. It follows from the linearity of equation (13) that its solution can be represented as the sum

$$L_\lambda(r,\Omega) = L_{\mathrm{bs},\lambda}(r,\Omega) + L_{\mathrm{rest},\lambda}(r,\Omega)\,. \qquad (17)$$

Here $L_{\mathrm{bs},\lambda}$ is the solution of the "black-soil problem" which satisfies equation (13) with boundary conditions expressed by equations (14), (15), and

$$L_{\mathrm{bs},\lambda}(r_\mathrm{b},\Omega) = 0, \quad r_\mathrm{b}\in\delta V_\mathrm{b}, \quad \Omega\bullet\mathrm{n}_\mathrm{b} < 0\,.$$

The function $L_{\mathrm{rest},\lambda}$ also satisfies equation (13) with F_λ=0 and boundary conditions expressed as

$$L_{\mathrm{rest},\lambda}(r_\mathrm{t},\Omega) = 0\,, \quad r_\mathrm{t}\in\delta V_\mathrm{t}\,, \quad \Omega\bullet\mathrm{n}_\mathrm{t} < 0\,,$$

$$L_{\mathrm{rest},\lambda}(r_\mathrm{l},\Omega) = \frac{1}{\pi}\int\limits_{\Omega'\bullet\mathrm{n}_\mathrm{l}>0} R_{\mathrm{l},\lambda}(\Omega',\Omega)L_{\mathrm{rest},\lambda}(r_\mathrm{l},\Omega')|\Omega'\bullet\mathrm{n}_\mathrm{l}|d\Omega', \qquad (18)$$

$$r_\mathrm{l}\in\delta V_\mathrm{l}\,, \quad \Omega\bullet\mathrm{n}_\mathrm{l} < 0\,,$$

$$L_{\mathrm{rest},\lambda}(r_\mathrm{b},\Omega) = \frac{1}{\pi}\int\limits_{\Omega'\bullet\mathrm{n}_\mathrm{b}>0} R_{\mathrm{b},\lambda}(\Omega',\Omega)L_\lambda(r_\mathrm{b},\Omega')|\Omega'\bullet\mathrm{n}_\mathrm{b}|d\Omega', \qquad (19)$$

$$r_\mathrm{b}\in\delta V_\mathrm{b}\,, \quad \Omega\bullet\mathrm{n}_\mathrm{b} < 0\,.$$

Note that $L_{\mathrm{rest},\lambda}$ depends on the solution of the "complete transport problem." The boundary condition (19) can be rewritten as

$$L_{\mathrm{rest},\lambda}(r_\mathrm{b},\Omega) = \rho_{q,\mathrm{eff}}(\lambda)S_q(r_\mathrm{b},\Omega)T_{q,\lambda}, \qquad (20)$$

where $\rho_{q,\mathrm{eff}}$ and S_q are defined by (2) and (5), respectively, and

$$T_{q,\lambda}(r_\mathrm{b}) = \int\limits_{2\pi-} q(\Omega')L_\lambda(r_\mathrm{b},\Omega')|\mu'|d\Omega'\,. \qquad (21)$$

The function q is defined by (3). The coefficient $\rho_{q,\mathrm{eff}}$ is assumed to be independent of the point r_b. It is taken as the parameter describing the reflectance of the surface underneath the canopy and can vary continuously within a biome-dependent interval (section 2). The biome-dependent function S_q is assumed to be wavelength independent and known (section 2). We replace $T_{q,\lambda}$ in (20) by its mean value over the ground surface. This implies that the variable $T_{q,\lambda}$ is independent on the space point r_b (this is automatically fulfilled if a one-dimensional radiative transfer model is used to evaluate the radiative field in plant canopies). Taking into account equation (20), we then can rewrite the solution of the transport problem, equation (17), as

$$L_\lambda(r,\Omega) = L_{\mathrm{bs},\lambda}(r,\Omega) + \rho_{q,\mathrm{eff}}(\lambda)T_{q,\lambda}L_{q,\lambda}(r,\Omega)\,, \qquad (22)$$

where $L_{q,\lambda}(r,\Omega)$ satisfies equation (13) with F_λ=0, boundary condition expressed by equation (18), and

$$L_{q,\lambda}(r_\mathrm{t},\Omega) = 0, \quad r_\mathrm{t}\in\delta V_\mathrm{t}, \quad \Omega\bullet\mathrm{n}_\mathrm{t} < 0\,, \qquad (23)$$

$$L_{q,\lambda}(r_\mathrm{b},\Omega) = S_q(r_\mathrm{b},\Omega), \quad r_\mathrm{b}\in\delta V_\mathrm{b}, \quad \Omega\bullet\mathrm{n}_\mathrm{b} < 0\,. \qquad (24)$$

Thus $L_{q,\lambda}(r,\Omega)$ describes the radiation regime in a plant canopy generated by anisotropic and heterogeneous sources $S(r_\mathrm{b},\Omega)$ located at the canopy bottom. We term the problem of finding $L_{q,\lambda}(r,\Omega)$ an "S problem." Substituting (22) in (21), we get

$$T_{q,\lambda}(r_\mathrm{b}) = T^q_{\mathrm{bs},\lambda}(r_\mathrm{b}) + \rho_{q,\mathrm{eff}}(\lambda)T_{q,\lambda}\mathbf{r}_{q,\lambda}(r_\mathrm{b})\,, \qquad (25)$$

where

$$T^q_{\mathrm{bs},\lambda}(r_\mathrm{b}) = \int\limits_{2\pi-} q(\Omega')L_{\mathrm{bs},\lambda}(r_\mathrm{b},\Omega')|\mu'|d\Omega'\,,$$

$$\mathbf{r}_{q,\lambda}(r_\mathrm{b}) = \int\limits_{2\pi-} q(\Omega')L_{q,\lambda}(r_\mathrm{b},\Omega')|\mu'|d\Omega'\,.$$

We then average equation (25) over the ground surface. This allows us to express $T_{q,\lambda}$ via $T^q_{\mathrm{bs},\lambda}$, $\mathbf{r}_{q,\lambda}$, and $\rho_{q,\mathrm{eff}}$. Substituting the averaged $T_{q,\lambda}$ into equation (22), we get

$$L_\lambda(r,\Omega) \approx L_{\mathrm{bs},\lambda}(r,\Omega) + \frac{\rho_{q,\mathrm{eff}}(\lambda)}{1-\rho_{q,\mathrm{eff}}(\lambda)\mathbf{r}_{q,\lambda}}T^q_{\mathrm{bs},\lambda}L_{q,\lambda}(r,\Omega). \qquad (26)$$

Here $T^q_{\mathrm{bs},\lambda}$ and $\mathbf{r}_{q,\lambda}$ are averages over the canopy bottom. Note that we can replace the approximate equality in equation (26) by an exact equality if a one-dimensional canopy radiation model is used to evaluate the radiative regime. It follows from equation (26) that the BHR, A^{hem}_λ, HDRF, r_λ, and the fraction of radiation absorbed by the vegetation, $\mathbf{a}^{\mathrm{hem}}_\lambda$, at wavelength λ can be expressed as

$$A^{\mathrm{hem}}_\lambda(\Omega_0) \approx \mathbf{r}^{\mathrm{hem}}_{\mathrm{bs},\lambda}(\Omega_0) + \mathbf{t}_{q,\lambda}\frac{\rho_{q,\mathrm{eff}}(\lambda)}{1-\rho_{q,\mathrm{eff}}(\lambda)\mathbf{r}_{q,\lambda}}\mathbf{t}^{\mathrm{hem},q}_{\mathrm{bs},\lambda}(\Omega_0), \qquad (27)$$

$$r_\lambda(\Omega,\Omega_0) \approx r_{\mathrm{bs},\lambda}(\Omega,\Omega_0) + \tau_{q,\lambda}(\Omega)\frac{\pi\rho_{q,\mathrm{eff}}(\lambda)}{1-\rho_{q,\mathrm{eff}}(\lambda)\mathbf{r}_{q,\lambda}}\mathbf{t}^{\mathrm{hem},q}_{\mathrm{bs},\lambda}(\Omega_0), \qquad (28)$$

$$\mathbf{a}^{\mathrm{hem}}_\lambda(\Omega_0) \approx \mathbf{a}^{\mathrm{hem}}_{\mathrm{bs},\lambda}(\Omega_0) + \mathbf{a}_{q,\lambda}\frac{\rho_{q,\mathrm{eff}}(\lambda)}{1-\rho_{q,\mathrm{eff}}(\lambda)\mathbf{r}_{q,\lambda}}\mathbf{t}^{\mathrm{hem},q}_{\mathrm{bs},\lambda}(\Omega_0), \qquad (29)$$

where $\mathbf{r}^{\mathrm{hem}}{}_{\mathrm{bs},\lambda}$, $\mathbf{a}^{\mathrm{hem}}{}_{\mathrm{bs},\lambda}$, and $r_{\mathrm{bs},\lambda}$ are the BHR, HDRF, and the fraction of radiation absorbed by the vegetation, respectively, when the canopy ground reflectance is zero. Here

$$\mathbf{t}^{\mathrm{hem},q}_{\mathrm{bs},\lambda}(\Omega_0) = \frac{T^q_{\mathrm{bs},\lambda}}{\int\limits_{2\pi-}|\mu'|L_\lambda(r_\mathrm{t},\Omega')d\Omega'}$$

is the weighted canopy transmittance,

$$\mathbf{t}_{q,\lambda} = \int_{2\pi^+} |\mu'| L_{q,\lambda}(r_1, \Omega') d\Omega'$$

is the transmittance resulting from the anisotropic source S_q located at the canopy bottom, and

$$\tau_{q,\lambda}(\Omega) = L_{q,\lambda}(r_1, \Omega)$$

is the radiance generated by S_q which leaves the top of the plant canopy, and $\mathbf{a}_{q,\lambda}$ is the radiance generated by S_q and absorbed by the vegetation. The radiation reflected, transmitted, and absorbed by the vegetation must be related via the energy conservation law,

$$\mathbf{r}_{\mathrm{bs},\lambda}^{\mathrm{hem}} + k_{q,\lambda}(\Omega_0)\mathbf{t}_{\mathrm{bs},\lambda}^{\mathrm{hem},q} + \mathbf{a}_{\mathrm{bs},\lambda}^{\mathrm{hem}} = 1, \tag{30}$$

$$k_{q,\lambda}(\Omega_0) = \frac{\mathbf{t}_{\mathrm{bs},\lambda}^{\mathrm{hem},q=\mathrm{l}}(\Omega_0)}{\mathbf{t}_{\mathrm{bs},\lambda}^{\mathrm{hem},q}(\Omega_0)},$$

$$\mathbf{r}_{q,\lambda} + \mathbf{t}_{q,\lambda} + \mathbf{a}_{q,\lambda} = 1. \tag{31}$$

Note that all the variables in equations (27) and (28) are mean values averaged over the top surface of the canopy.

It follows from equation (27) that

$$A_\lambda^{\mathrm{hem}}(\Omega_0) - \mathbf{r}_{\mathrm{bs},\lambda}^{\mathrm{hem}}(\Omega_0) \approx \mathbf{t}_{q,\lambda} \frac{\rho_{q,\mathrm{eff}}(\lambda)}{1 - \rho_{q,\mathrm{eff}}(\lambda)\mathbf{r}_{q,\lambda}} \mathbf{t}_{\mathrm{bs},\lambda}^{\mathrm{hem},q}(\Omega_0). \tag{32}$$

Thus the contribution of the ground to the canopy-leaving radiance is proportional to the square of canopy transmittance and that the factor of proportionality depends on $\rho_{q,\mathrm{eff}}$. If the right-hand side is sufficiently small, we can neglect this contribution by assigning a value of zero to the effective soil reflectance.

Thus we have parameterized the solution of the transport problem in terms of $\rho_{q,\mathrm{eff}}$ and solutions of the "black-soil problem" and "S problem." The solution of the "black-soil problem" depends on Sun-view geometry, canopy architecture, and spectral properties of the leaves. The "S problem" depends on spectral properties of the leaves and canopy structure only. At this stage, these properties allow a significant reduction in the size of the LUT because there is no need to store the dependence of the exiting radiation field on ground reflection properties. Since the solution of the "black-soil problem" and "S problem" determine the size of the LUT, we focus on the solution of these problems, using equation (26) as the basis of the algorithm. The next step is to specify the wavelength dependence of the basic algorithm equation.

5. Spectral Variation of Canopy Absorptance, Transmittance, and Reflectance for Conservative Models

Let us consider equation (11) with boundary conditions expressed by equations (14)-(16). This boundary value problem can be reduced to the solution of the "black-soil problem" and "S problem." In the LAI/FPAR retrieval algorithm the boundary conditions (15) for the lateral surface of domain V are replaced by vacuum condition, i.e., $L_\lambda(r_1,\Omega)=0$ if $r_1 \in \delta V_1$ and $\Omega \bullet \mathrm{n}_1 < 0$ [*Diner et al.*, 1998b; *Knyazikhin* et al., this issue]. The boundary condition of the "S problem" expressed by equations (18), (23), and (24) are wavelength independent in this case. The incoming radiation (14) can be parameterized in terms of two scalar values: $f_{\mathrm{dir},\lambda}$ and total flux $F_{0,\lambda}$ of incoming radiation. It allows representing the "black-soil problem" as a sum of two radiation fields. The first is generated by the monodirectional component of solar radiation incident on the top surface of the canopy boundary and, the second, by the diffuse component. Dividing the transport equations and boundary conditions which define these problems by $f_{\mathrm{dir},\lambda}F_{0,\lambda}$ and $(1-f_{\mathrm{dir},\lambda})F_{0,\lambda}$, one can reduce them to transport problems with wavelength-independent boundary conditions. Thus the spectral variation of the radiative field in vegetation canopies can be described, when the spectral variation of the solution of the transport equation with wavelength-independent boundary conditions is known. Therefore we consider the following boundary value problem for the transport equation

$$\Omega \bullet \nabla \varphi_\lambda(r,\Omega) + \sigma(r,\Omega)\varphi_\lambda(r,\Omega) = \int_{4\pi} \sigma_{\mathrm{s},\lambda}(r,\Omega' \to \Omega)\varphi_\lambda(r,\Omega')d\Omega', \tag{33}$$

$$\varphi_\lambda(r,\Omega) = B(r,\Omega), \qquad r \in \delta V, \qquad \mathrm{n}_r \bullet \Omega < 0. \tag{34}$$

Here B is a wavelength-independent function defined on the canopy boundary δV, and n_r is the outward normal at the point $r \in \delta V$. Differentiating equations (33) and (34) with respect to wavelength λ, we get

$$\Omega \bullet \nabla u_\lambda(r,\Omega) + \sigma(r,\Omega)u_\lambda(r,\Omega) = \frac{d}{d\lambda}\int_{4\pi} \sigma_{\mathrm{s},\lambda}(r,\Omega' \to \Omega)\varphi_\lambda(r,\Omega')d\Omega', \tag{35}$$

$$u_\lambda(r,\Omega) = 0, \qquad r \in \delta V, \qquad \mathrm{n}_r \bullet \Omega < 0, \tag{36}$$

where

$$u_\lambda(r,\Omega) = \frac{d\,\varphi(r,\Omega)}{d\,\lambda}.$$

The following results from eigenvector theory are required to derive a relationship between spectral leaf albedo and canopy absorptance, transmittance, and reflectance.

An eigenvalue of the transport equation is a number γ such that there exists a function φ which satisfies

$$\gamma[\Omega \bullet \nabla\varphi(r,\Omega) + \sigma(r,\Omega)\varphi(r,\Omega)] = \int_{4\pi} \sigma_{\mathrm{s},\lambda}(r,\Omega' \to \Omega)\varphi(r,\Omega')d\Omega', \tag{37}$$

with boundary conditions

$$\varphi(r,\Omega)=0, \quad r \in \delta V = \delta V_{\mathrm{t}} + \delta V_{\mathrm{b}} + \delta V_{\mathrm{l}}, \quad \mathrm{n}_r \bullet \Omega < 0.$$

The function $\varphi(r,\Omega)$ is termed an eigenvector corresponding to the given eigenvalue γ.

The set of eigenvalues γ_k, k=0,1,2, ... and eigenvectors $\varphi_k(r,\Omega)$, k=0,1,2, ... of the transport equation is a discrete set [*Vladimirov*, 1963]. The eigenvectors are mutually orthogonal; that is,

$$\int_V \int_{4\pi} \sigma(r,\Omega)\varphi_k(r,\Omega)\varphi_l(r,\Omega)\,d\Omega\,dr = \delta_{k,l} \qquad (38)$$

where $\delta_{k,l}$ is the Kroneker symbol. The transport equation has a unique positive eigenvalue which corresponds to a unique positive (normalized in the sense of equation (38)) eigenvector [*Germogenova*, 1986]. This eigenvalue is greater than the absolute magnitudes of the remaining eigenvalues. This means that only one eigenvector, say φ_0, takes on positive values for any $r \in V$ and Ω. This positive couplet of eigenvector and eigenvalue plays an important role in transport theory, for instance, in neutron transport theory. This positive eigenvalue alone determines if the fissile assembly will function as a reactor, or as an explosive, or will melt. Its value successfully relates the reactor geometry to the absorption capacity of the active zone. Because the reactor is controlled by changing the absorption capacity of the active zone (by inserting or removing absorbents), this value is critical to its functioning. The similarity to the problem at hand is that we need to relate canopy architecture ("similar" to reactor geometry) with leaf optical properties ("similar" to the absorption capacity of the active zone). The expansion of the solution of the transport equation in eigenvectors has mainly a theoretical value because the problem of finding these vectors is much more complicated than finding the solution of the transport equation. However, this approach can be useful if we want to estimate some integrals of the solution. Therefore we apply this technique to derive a relationship between spectral leaf albedo and canopy absorptance, transmittance, and reflectance.

Equation (35) with boundary conditions (36) is a linear homogeneous differential equation with respect to λ in a functional space [*Krein*, 1972]. Its solution φ can be expanded in eigenvectors,

$$\varphi_\lambda(r,\Omega) = a_0(\lambda)\varphi_0(\lambda,r,\Omega) + \sum_{k=1}^{\infty} a_k(\lambda)\varphi_k(\lambda,r,\Omega), \quad (39)$$

where coefficients a_k do not depend on spatial or angular variables. Here we separate the positive eigenvector φ_0 into the first summand. As described above, only this summand, $a_0\varphi_0$, takes on positive values for any $r \in V$ and Ω. Substituting (39) into equation (35), we get

$$\sum_{k=0}^{\infty} [\Omega \bullet \nabla u_k(\lambda,r,\Omega) + \sigma(r,\Omega)u_k(\lambda,r,\Omega)]$$

$$= \sum_{k=0}^{\infty} \frac{d}{d\lambda} \int_{4\pi} \sigma_{s,\lambda}(r,\Omega' \to \Omega) a_k \varphi_k(\lambda,r,\Omega')\,d\Omega', \qquad (40)$$

where $u_k = d(a_k\varphi_k)/d\lambda$. Substituting (37) into (40), further results in

$$\sum_{k=0}^{\infty} [\Omega \bullet \nabla + \sigma(r,\Omega)]$$

$$\times \left\{ [1-\gamma_k(\lambda)]u_k(\lambda,r,\Omega) - a_k(\lambda)\varphi_k(\lambda,r,\Omega)\frac{d\gamma_k(\lambda)}{d\lambda} \right\} = 0.$$

Here $\gamma_k(\lambda)$ is the eigenvalue corresponding to the eigenvector φ_k. It follows from this equation, as well as from the orthogonality of eigenvectors, that

$$\frac{d[a_k(\lambda)\varphi_k(\lambda,r,\Omega)]}{d\lambda} = \frac{\frac{d\gamma_k(\lambda)}{d\lambda}}{1-\gamma_k(\lambda)} [a_k(\lambda)\varphi_k(\lambda,r,\Omega)].$$

Solving this ordinary differential equation results in

$$a_k(\lambda)\varphi_k(\lambda,r,\Omega) = \frac{1-\gamma_k(\lambda_0)}{1-\gamma_k(\lambda)} [a_k(\lambda_0)\varphi_k(\lambda_0,r,\Omega)]. \quad (41)$$

Thus if we know the kth summand of the expansion in equation (39) at a wavelength λ_0, we can easily find this summand for any other wavelength.

We introduce $\mathbf{e}$, the monochromatic radiation at wavelength λ intercepted by the vegetation canopy,

$$\mathbf{e}(\lambda) = \int_V dr \int_{4\pi} d\Omega \sigma(r,\Omega)\varphi_\lambda(r,\Omega), \qquad (42)$$

and $\mathbf{e}_0$ as

$$\mathbf{e}_0(\lambda) = \int_V \int_{4\pi} \sigma(r,\Omega)\varphi_\lambda(r,\Omega) \cdot \varphi_0(\lambda,r,\Omega)\,dr\,d\Omega. \quad (43)$$

Given $\mathbf{e}$, we can evaluate the fraction $\mathbf{a}$ of radiation absorbed by the vegetation at the wavelength λ as

$$\mathbf{a}(\lambda) = [1-\omega(\lambda)]\mathbf{e}(\lambda), \qquad (44)$$

where

$$\omega(\lambda) = \frac{1}{\pi} \frac{\int_{4\pi} \Gamma_\lambda(r,\Omega' \to \Omega)\,d\Omega}{G(r,\Omega')} \qquad (45)$$

is the leaf albedo. Below an estimation of $\mathbf{e}_0$ will be performed. This value is close to $\mathbf{e}$. We skip a precise mathematical proof of this fact here. An intuitive explanation is as follows: Putting (39) in (42) and integrating the series results in only the positive term containing $a_0\varphi_0$. As a result, $\mathbf{e}(\lambda)/\mathbf{e}(\lambda_0) \approx \mathbf{e}_0(\lambda)/\mathbf{e}_0(\lambda_0)$. Let us derive the dependence of $\mathbf{e}$ on wavelength. Substituting equation (39) into equation (43) and taking into account equation (41) as well as the orthogonality of eigenvectors, equation (38), we obtain

$$\mathbf{e}_0(\lambda) = \frac{1-\gamma_0(\lambda_0)}{1-\gamma_0(\lambda)} \mathbf{e}_0(\lambda_0),$$

where γ_0 is the positive eigenvalue corresponding to the positive eigenvector φ_0. Taking into account equation (44), we can also derive the following estimation for $\mathbf{a}$:

$$\mathbf{a}(\lambda) = \frac{1-\gamma_0(\lambda_0)}{1-\gamma_0(\lambda)} \cdot \frac{1-\omega(\lambda)}{1-\omega(\lambda_0)} \mathbf{a}(\lambda_0). \qquad (46)$$

Thus given canopy absorptance at wavelength λ_0, we can evaluate this variable at any other wavelength. Figure 2 shows spectral variation of the fraction of energy absorbed by the vegetation canopy **a** for uniform and planophile leaves. Equation (46) can also be used to specify the accuracy of a canopy radiation model to simulate the radiative field in the canopy. On can see (Figure 2, right) that our radiation model is erroneous in the case of planophile leaves when LAI>5 and the leaf albedo ω>0.5. At a given wavelength, **a** is a function of canopy structure and Sun position in the case of "black-soil problem," and a function of canopy structure only in the case of the "*S* problem." We store **a** at a fixed wavelength λ_0 in the LUT.

A somewhat more complicated technique is realized to derive an approximation for canopy transmittance,

$$\mathbf{t}\left(\lambda, \frac{r_{D,\lambda}}{\omega(\lambda)}\right) = \frac{1-\gamma_0(\lambda_0)}{1-\gamma_0(\lambda)}\,\mathbf{t}\left(\lambda_0, \frac{r_{D,\lambda}}{\omega(\lambda)}\right), \qquad (47)$$

where $r_{D,\lambda}$ is the spectral reflectance of the leaf element. The ratio $r_{D,\lambda}/\omega(\lambda)$ is assumed to be constant with respect to wavelength for each biome. Thus given the canopy transmittance at wavelength λ_0, we can evaluate this variable for wavelength λ. Figure 3 shows spectral variation of canopy transmittance for uniform leaves evaluated with our canopy radiation model and with equation (47). At a fixed wavelength, **t** is a function of canopy structure and Sun position in the case of the "black-soil problem," and a function of canopy structure in the case of the "*S* problem." We store **t** at a fixed wavelength λ_0 in the LUT.

The canopy reflectance **r** is related to the absorptance and transmittance via the energy conservation principle

$$\mathbf{r}(\lambda) = 1 - \mathbf{t}(\lambda) - \mathbf{a}(\lambda). \qquad (48)$$

Thus given canopy transmittance and absorptance at a fixed wavelength, we can obtain the canopy reflectance for any wavelength. Figure 4 demonstrates an example of equation (48).

The unique positive eigenvalue γ_0, corresponding to the unique positive eigenvector, can be estimated as [*Knyazikhin and Marshak*, 1991]

$$\gamma_0(\lambda) = \omega(\lambda)[1 - \exp(-K)], \qquad (49)$$

where K is a coefficient which may depend on canopy structure (i.e., biome type, LAI, ground cover, etc.) and Sun position but not on wavelength or soil type. Its specification depends on the parameter (absorptance or transmittance) and type of transport problem ("black-soil problem" or "*S* problem"). The coefficient K, however, does not depend on the transport problem and sun position, when it refers to canopy absorptance. Figure 5 shows the coefficient K for the "*S* problem" and canopy absorptance as a function of LAI. This coefficient is an element of the LUT. Note that the eigenvalue γ_0 depends on values of spectral leaf albedo (45) which, in turn, depends on wavelength. It allows us to parameterize canopy absorptance, transmittance, and reflectance in terms of canopy structure, Sun position and leaf albedo.

6. Constraints on Look-Up Table Entries

In spite of the diversity of canopy reflectance models, their direct use in an inversion algorithm is ineffective. In the case of forests, for example, the interaction of photons with the rough and rather thin surface of tree crowns and with the ground in between the crowns are the most important factors causing the observed variation in the directional reflectance distribution. These phenomena are rarely captured by many canopy reflectance models. As a result, these models are only slightly sensitive to the within-canopy radiation regime. This assertion is based on the fact that a rather wide family of canopy radiation models are solutions to (13), including models with a nonphysical internal source F_λ (Appendix).

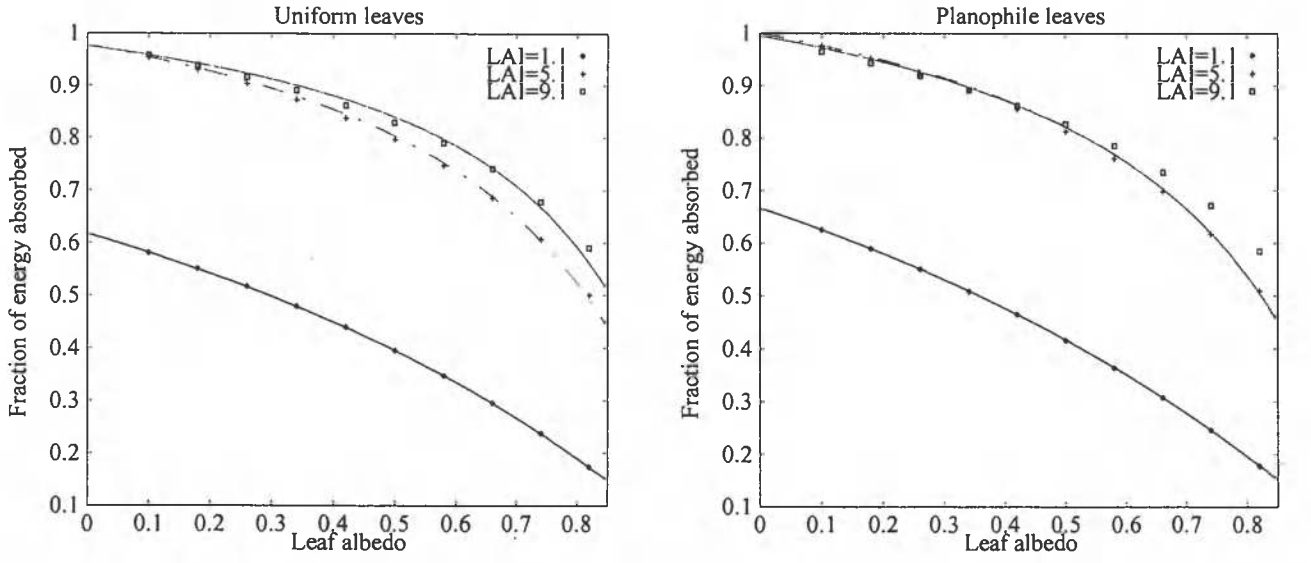

Figure 2. Spectral variation of fraction of absorbed radiation by vegetation for uniform (left) and planophile (right) leaves evaluated with canopy radiation model (points) and from equation (46).

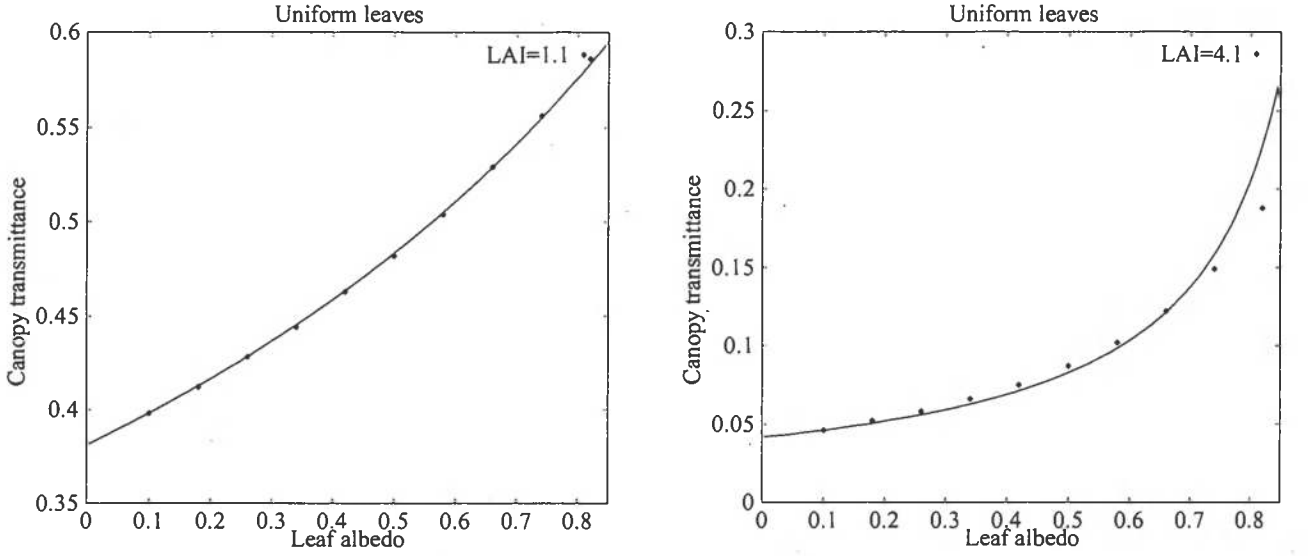

Figure 3. Spectral variation canopy transmittance for uniform leaves evaluated with canopy radiation model (points) and from equation (47) for LAI=1.1 (left) and 4.1 (right).

Within such a model the sum of radiation absorbed, transmitted, and reflected by the canopy are not equal to the radiation incident on the canopy. The function F_λ is chosen such that the model simulates the reflected radiation field correctly, i.e., these models account for photon interactions within a rather small domain of the vegetation canopy. On the other hand, it is the within-canopy radiation regime that is very sensitive to the canopy structure and therefore to LAI. The within-canopy radiation regime also determines the amount of solar energy absorbed by the vegetation. Ignoring this phenomenology in canopy radiation models leads to a large number of nonphysical solutions when one inverts a canopy reflectance model. Therefore (27) and (28) must be transformed before they can be used in a retrieval algorithm.

Let us introduce the required weights

$$w_{\mathrm{bs},\lambda}(\Omega,\Omega_0)=\frac{\pi^{-1}r_{\mathrm{bs},\lambda}(\Omega,\Omega_0)}{\mathbf{r}^{\mathrm{hem}}_{\mathrm{bs},\lambda}(\Omega_0)},\quad \int_{2\pi^+} w_{\mathrm{bs},\lambda}(\Omega,\Omega_0)|\mu|d\Omega=1, \tag{50}$$

$$w^q_\lambda(\Omega)=\frac{\tau_{q,\lambda}(\Omega)}{\mathbf{t}_{q,\lambda}},\qquad \int_{2\pi^+} w^q_\lambda(\Omega)|\mu|d\Omega=1, \tag{51}$$

With this notation, (28) can be rewritten as

$$r_\lambda(\Omega,\Omega_0)\approx \pi w_{\mathrm{bs},\lambda}\mathbf{r}^{\mathrm{hem}}_{\mathrm{bs},\lambda}(\Omega_0)+\pi w^q_\lambda \mathbf{t}_{q,\lambda}\frac{\rho_{q,\mathrm{eff}}(\lambda)}{1-\rho_{q,\mathrm{eff}}(\lambda)\mathbf{r}_{q,\lambda}}\mathbf{t}^{\mathrm{hem},q}_{\mathrm{bs},\lambda}(\Omega_0) \tag{52}$$

and from (30) and (31), the canopy reflectances $\mathbf{r}^{\mathrm{hem}}_{\mathrm{bs},\lambda}$ and $\mathbf{r}_{q,\lambda}$ can be written as

$$\mathbf{r}^{\mathrm{hem}}_{\mathrm{bs},\lambda}=1-\mathbf{t}^{\mathrm{hem},q=1}_{\mathrm{bs},\lambda}-\mathbf{a}^{\mathrm{hem}}_{\mathrm{bs},\lambda}, \tag{53}$$

$$\mathbf{r}_{q,\lambda}=1-\mathbf{t}_{q,\lambda}-\mathbf{a}_{q,\lambda}. \tag{54}$$

Thus (52) is sensitive to both factors determining the directional reflectance distribution of plant canopies (the weight $w_{\mathrm{bs},\lambda}$) and to the within-canopy radiation regime $[\mathbf{t}^{\mathrm{hem},q=1}_{\mathrm{bs},\lambda}, \mathbf{a}^{\mathrm{hem}}_{\mathrm{bs},\lambda}, \mathbf{t}_{q,\lambda}, \mathbf{a}_{q,\lambda}]$. Equations (52)-(54) also allow the formulation of a test for the "eligibility" of a canopy radiation model to generate the LUT. First the weights $w_{\mathrm{bs},\lambda}$ are evaluated as a function of Sun-view geometry, wavelength, and LAI by using a field-tested canopy reflectance model. Then with the same model, $\mathbf{r}^{\mathrm{hem}}{}_{\mathrm{bs},\lambda}$ and $\mathbf{r}_{q,\lambda}$ are evaluated from (53) and (54), and inserted into (52). A canopy radiation model is "eligible" to generate the LUT file if (50) and (51) are satisfied to within a given accuracy for any Sun-view combination, wavelength, and LAI. We do not know of a

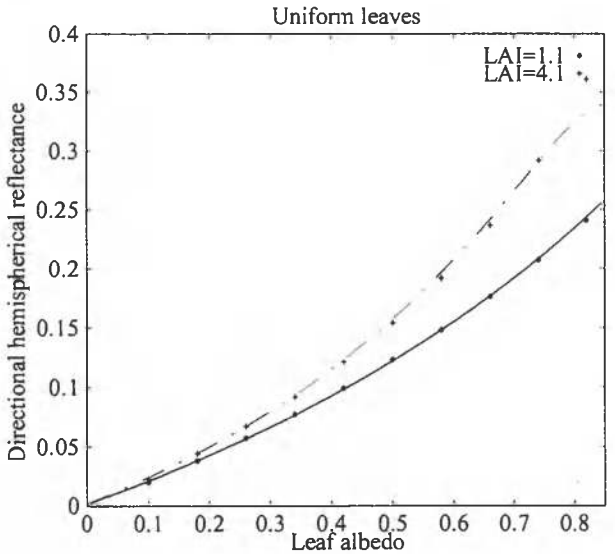

Figure 4. Spectral variation of the DHR for uniform leaves evaluated with canopy radiation model (points) and from equation (48) for LAI=1.1 and 4.1.

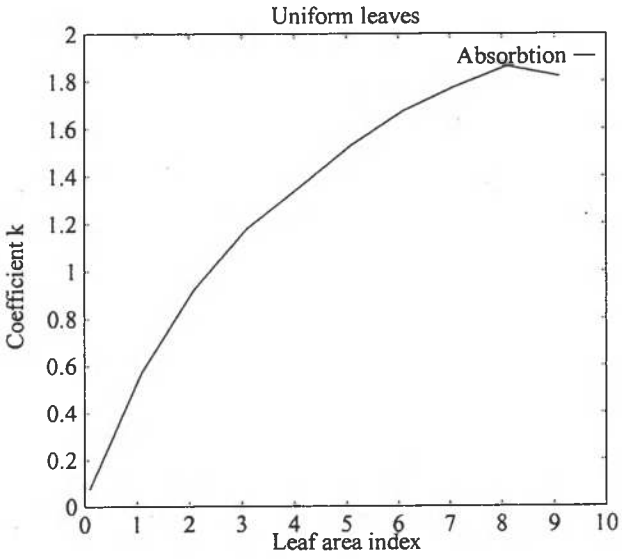

Figure 5. Coefficient K as a function of LAI for canopy absorptance.

canopy reflectance model which can pass the above test. That is because there is no published model thus far which satisfies the energy conservation law. Although a conservative transport equation for a vegetation canopy has not yet been formulated, solutions of this equation satisfy properties derived in a previous section. These properties can be used to correct existing canopy radiation models for the "eligibility" to generate the LUT. An algorithm to correct a canopy radiation model is presented by *Knyazikhin et al.* [this issue] which was used to generate the LUT for the MISR LAI/FPAR retrieval algorithm.

It follows from (32) and (52) that the HDRF can be represented as

$$r_\lambda(\Omega,\Omega_0) \approx \pi w_{bs,\lambda} \mathbf{r}^{hem}_{bs,\lambda}(\Omega_0) + w^q_\lambda [A^{hem}_\lambda(\Omega_0) - \mathbf{r}^{hem}_{bs,\lambda}(\Omega_0)]. \quad (55)$$

For each pixel the MISR instrument provides the spectral BHR and DHR. Therefore this expression is used to evaluate the HDRF and BRF in the case of MISR data, setting retrieved A^{hem}_λ in (55). Equation (28) is used to evaluate the BRF in the case of MODIS data.

Thus the BHR described by (27) and the HDRF described by (55) can be expressed in terms of optical properties of a leaf and the energy conservation law, as well as in terms of solutions of the "black-soil problem" and "S problem" at a reference leaf albedo value of $\omega(\lambda_0)$. This facilitates comparison of spectral values of the BHR or HDRF with spectral properties of individual leaves, which is a rather stable characteristic of a green leaf. It also can be interpreted as "inclusion of additional information" into the algorithm, thus allowing a significant reduction in the number of retrieved solutions. Canopy transmittances and absorptances, and coefficients $\mathbf{p}$=1-exp(-K) where K is defined by (49) for the "black-soil problem" and "S problem" at a reference leaf albedo value of ω^* as well as the weights (50) and (51) are precomputed and stored in the LUT. It allows the use of the same LUT for MODIS and MISR instruments. A detailed description of such a LUT is presented by *Diner et al.* [1998b].

7. LAI Retrieval From MODIS and MISR Data

For each pixel the MODIS instrument can provide atmosphere-corrected BRF in one view direction and at seven bands in the solar spectrum every day [*Vermote et al.*, 1995]. The MISR instrument covers the whole globe within 8 days. For each pixel, it provides the HDRF, BHR, BRF, and DHR in nine view directions and at four spectral bands of solar spectrum [*Diner et al.*, 1998a; *Martonchik et al.*, 1998]. Thus every 8 days, one has the set of pixel reflectances corresponding to 16 different Sun positions, 15 view angles, and at 11 spectral bands. These canopy reflectances and Sun-view geometry are input for the algorithm. Note that this is the maximum amount of information which may be available. In reality, however, it may be less, e.g., because of cloud cover and performance of preprocessing algorithms. Let $r_{0,\lambda}(\Omega',\Omega'_0)$ be the BRF retrieved from MODIS data and $r_\lambda(\Omega,\Omega_0)$ and $A^{hem}_\lambda(\Omega_0)$ be the BRF and BHR retrieved from MISR data. Here Ω' and Ω are the view MODIS and MISR directions, Ω'_0 and Ω_0 are the direction of direct solar radiation during times of MODIS and MISR observations, and β, λ denote the center of the MODIS and MISR spectral bands, respectively. These retrieved reflectances are the input for the algorithm which we express in the vector-matrix form as

$$\bar{r}_0 = \begin{pmatrix} r_{0,\beta_1}(\Omega'_1,\Omega'_{0,1}) & r_{0,\beta_1}(\Omega'_2,\Omega'_{0,2}) & \cdots & r_{0,\beta_7}(\Omega'_8,\Omega'_{0,8}) \\ r_{0,\beta_2}(\Omega'_1,\Omega_{0,1}) & r_{0,\beta_2}(\Omega'_2,\Omega'_{0,2}) & \cdots & r_{0,\beta_2}(\Omega'_8,\Omega'_{0,8}) \\ \vdots & \vdots & \vdots & \vdots \\ r_{0,\beta_7}(\Omega'_1,\Omega'_{0,1}) & r_{0,\beta_7}(\Omega'_2,\Omega'_{0,2}) & \cdots & r_{0,\beta_7}(\Omega'_8,\Omega'_{0,8}) \end{pmatrix},$$

$$\bar{r}(\Omega_0)$$

$$= \begin{pmatrix} r_{\lambda 1}(\Omega_1,\Omega_0) & r_{\lambda 2}(\Omega_1,\Omega_0) & r_{\lambda 3}(\Omega_1,\Omega_0) & r_{\lambda 4}(\Omega_1,\Omega_0) \\ r_{\lambda 1}(\Omega_2,\Omega_0) & r_{\lambda 2}(\Omega_2,\Omega_0) & r_{\lambda 3}(\Omega_2,\Omega_0) & r_{\lambda 4}(\Omega_2,\Omega_0) \\ \vdots & \vdots & \vdots & \vdots \\ r_{\lambda 1}(\Omega_9,\Omega_0) & r_{\lambda 2}(\Omega_9,\Omega_0) & r_{\lambda 3}(\Omega_9,\Omega_0) & r_{\lambda 4}(\Omega_9,\Omega_0) \end{pmatrix},$$

$$\bar{A}^{hem}(\Omega_0)$$

$$= \left[A^{hem}_{\lambda 1}(\Omega_0) \quad A^{hem}_{\lambda 2}(\Omega_0) \quad A^{hem}_{\lambda 3}(\Omega_0) \quad A^{hem}_{\lambda 4}(\Omega_0)\right].$$

Here β_k, k=1, 2, ... ,7 and λ_m, m=1,2,3,4 are centers of the MODIS and MISR spectral bands listed in Table 2. We will use $r_{0,\lambda}(\Omega,\Omega_0)$, $r_\lambda(\Omega,\Omega_0)$, $A^{hem}_\lambda(\Omega_0)$, $\bar{r}_0$, $\bar{r}(\Omega_0)$, and $\bar{A}^{hem}(\Omega_0)$ to denote modeled canopy reflectances (i.e., evaluated from equation (52) for MODIS and equations (55) and (27) for MISR instruments) and $\tilde{r}_{0\lambda}(\Omega,\Omega_0)$, $\tilde{r}_\lambda(\Omega,\Omega_0)$, $\tilde{A}^{hem}{}_\lambda(\Omega)$, $\tilde{\bar{r}}_0$, $\tilde{\bar{r}}(\Omega_0)$, and $\tilde{\bar{A}}^{hem}(\Omega_0)$ to denote observations of these variables.

To establish relationships between measured surface reflectances and canopy structure, we introduce the space of canopy realization P. This space is represented by canopy structural types of global vegetation (biome), each represent-

ing patterns of the architecture of an individual tree and the entire canopy, and spectral leaf albedo (45) at MODIS and MISR bands. Each biome is characterized by ground cover g, mean LAI of an individual tree L, and pattern of effective ground reflectances (ρ_1, ρ_2, ..., ρ_{11}) in the MODIS and MISR bands (section 2). The element p of this space is the vector $p=(bio, \omega_1, \omega_2, \ldots, \omega_{11}, \rho_1, \rho_2, \ldots, \rho_{11}, L, g)$. Here bio can take six values only; one pattern ($\omega_1, \omega_2, \ldots, \omega_{11}$) of the spectral leaf albedo per biome. Ground cover, the LAI of individual vegetation, and effective ground reflectance can vary within given biome-dependent ranges (section 2). Thus the space of canopy realization is supposed to represent patterns of existing vegetation canopies. The set P is the sum of six biome-dependent subsets; that is,

$$P = \bigcup_{bio=1}^{6} P_{bio}.$$

The element of P_{bio} is the vector (ρ_1, ρ_2,..., ρ_{11}, L, g).

For each biome type, the modeled reflectances $\bar{r}_0$, $\bar{r}(\Omega_0)$, and $\bar{A}^{hem}(\Omega_0)$ are functions of p. In order to characterize the closeness between modeled and retrieved reflectances, the following merit functions are introduced

$$\Delta_0\left[\bar{r}_0, \tilde{\bar{r}}_0\right] = \frac{\sum_{l=1}^{7}\sum_{j=1}^{8} v_0(l,j)\left[\frac{r_{\beta_l}(\Omega'_j,\Omega'_{0,j}) - \tilde{r}_{\beta_l}(\Omega'_j,\Omega'_{0,j})}{\sigma_0(l,j)}\right]^2}{\sum_{i=1}^{7}\sum_{j=1}^{8} v_0(l,j)},$$

$$\Delta_r\left[\bar{r}(\Omega_0), \tilde{\bar{r}}(\Omega_0)\right] = \frac{\sum_{l=1}^{4}\sum_{j=1}^{9} v_r(l,j)\left[\frac{r_{\lambda_l}(\Omega_j,\Omega_0) - \tilde{r}_{\lambda_l}(\Omega_j,\Omega_0)}{\sigma_r(l,j)}\right]^2}{\sum_{i=1}^{4}\sum_{j=1}^{9} v_r(l,j)},$$

$$\Delta_A\left[\bar{A}^{hem}(\Omega_0), \tilde{\bar{A}}^{hem}(\Omega_0)\right] = \frac{\sum_{l=1}^{4} v_A(l)\left[\frac{A^{hem}_{\lambda_l}(\Omega_0) - \tilde{A}^{hem}_{\lambda_l}(\Omega_0)}{\sigma_A(l)}\right]^2}{\sum_{l=1}^{4} v_A(l)}. \quad (56)$$

The first and second functions characterize the closeness between modeled BRFs and those obtained from MODIS and MISR data. The third function compares modeled and retrieved BHRs. Here $v_0(l,j)$ and $v_r(l,j)$ take on the value 1 if the BRF at wavelength β_l and λ_l, in Sun-sensor directions $(\Omega'_j,\Omega'_{0,j})$ and (Ω_j,Ω_0), exists, and zero otherwise; $v_A(l)=1$ if the BHR at wavelength λ_l exists, and 0 otherwise; σ_0, σ_r, and σ_A are uncertainties in the BRFs and BHR retrievals. Thus the merit functions are defined and normalized such that a model which differs from the retrieved canopy reflectance values by an amount equivalent or less than the retrieval uncertainty will result in values of Δ_0, Δ_r, and Δ_A of the order of unity. In terms of these notations we formulate the inverse problem as follows: given biome type, bio, and atmosphere corrected canopy reflectances $\tilde{\bar{r}}_0$, $\tilde{\bar{r}}(\Omega_0)$, and $\tilde{\bar{A}}^{hem}(\Omega_0)$ find all $p \in P_{bio}$ for which $\Delta(p) \le h$ where h is a configurable threshold value and

$$\Delta(p) = \Delta_0\left[\bar{r}_0, \tilde{\bar{r}}_0\right] + \Delta_r\left[\bar{r}(\Omega_0), \tilde{\bar{r}}(\Omega_0)\right] + \Delta_A\left[\bar{A}^{hem}(\Omega_0), \tilde{\bar{A}}(\Omega_0)\right].$$

Any $p \in P_{bio}$ for which $\Delta(p) \le h$ must be considered a candidate for a true p. Let us introduce a set of candidates for the solution as

$$Q(L; P_{bio}) = \left\{p \in P_{bio} : LAI_0 \cdot g < L \text{ and } \Delta(p) \le h\right\}.$$

This set is subset of P_{bio} and contains such p from P_{bio} for which the leaf area index $LAI=LAI_0 \cdot g$ is less than a given value L from the interval $[L_{min} \cdot g_{min}, L_{max} \cdot g_{max}]$ and $\Delta(p) \le h$. The set $Q(L_{max} \cdot g_{max}; P_{bio})$ contains all $p \in P_{bio}$ for which a canopy radiation model generates output comparable with measured data.

In order to quantify acceptable candidates for the solution, we introduce measures (distribution functions) defined on the set P_{bio} as follows [*Knyazikhin et. al.*, this issue]. The subset P_{bio} is represented as a sum of nonintersected subsets

$$P_{bio} = \bigcup_{k=1}^{N} P_{bio,k}, \quad P_{bio,k} \cap P_{bio,j} = \varnothing, k \ne j.$$

Let $N(L;P_{bio})$ be numbers of subsets $P_{bio,k}$ containing at least one element from the set $Q(L;P_{bio})$. As measures of $Q(L;P_{bio})$, we introduce biome specific function $F_{bio}(L)$ as

$$F_{bio}(L) = \lim_{N\to\infty} \frac{N(L; P_{bio})}{N(L_{max} \cdot g_{max}; P_{bio})}. \quad (57)$$

The subset $P_{bio,k}$ specifies a set of canopy realizations whose range of variation is "sufficiently small." $N(L_{max} \cdot g_{max}; P_{bio})$ is total number of solutions of $\Delta(p) \le h$; $N(L;P_{bio})$ is the number of these solutions when the leaf area index $LAI_0 \cdot g$ is less then a given value L in the interval $[L_{min} \cdot g_{min}, L_{max} \cdot g_{max}]$. The function (57) is the LAI conditional distribution function provided $p \in P_{bio}$ and $\Delta(p) \le h$. Note that the function (57) depends on L, $\tilde{A}^{hem}{}_{\lambda}(\Omega_0)$, $\tilde{\bar{r}}_0$, $\tilde{\bar{r}}(\Omega_0)$, and $\tilde{\bar{A}}^{hem}(\Omega_0)$. The value

$$L_{bio} = \int_{L_{min} \cdot g_{min}}^{L_{max} \cdot g_{max}} l \, dF_{bio}(l)$$

is taken as solutions of $\Delta(p) \le h$ and the value

$$d^2_{bio} = \int_{L_{min} \cdot g_{min}}^{L_{max} \cdot g_{max}} (L_{bio} - l)^2 \, dF_{bio}(l) \quad (58)$$

is taken as the characteristic of the solution accuracy. Biome type bio is expected to be derived from the MODIS land cover product. Therefore the synergistic LAI/FPAR algorithm must have interfaces with MODIS/MISR reflectances product and the MODIS land cover product. If the inverse problem has no

solutions (i.e., F_{bio}=0), we assign a default value to (58) and a backup algorithm is triggered to estimate LAI using vegetation indices [*Myneni et al.*, 1997b]. Plate 1 demonstrates an example of prototyping of the LAI/FPAR algorithm with atmospherically corrected SeaWiFS (sea-viewing wide field-of-view sensor) data. The functions v_r and v_A were set to zero.

Given $\tilde{\bar{r}}_0$, $\tilde{\bar{r}}_0(\Omega_0)$, and $\tilde{\bar{A}}(\Omega_0)$, it may be the case that LAI algorithm admits a number of solutions, covering a wide range of LAI values. When this happens, the retrieved reflectances are said to belong to the saturation domain [*Knyazikhin et. al.*, this issue], being insensitive to the various parameter values of P_{bio}. Under this condition, the function (57), which describes the number of times a solution has a particular LAI value, will appear flat over the range of LAI, illustrating that the solutions all have equal probability of occurrence. Here we skip a description of this situation and how this situation can be quantified. For details of these results as well as a precise mathematical investigation of this approach and some numerical examples illustrating its various aspects, the reader is referred to [*Knyazikhin et. al.*, this issue].

8. Description of Synergistic FPAR Retrieval

It follows from (29) and (32) that the fractional amount of incident photosynthetically active radiation (PAR) absorbed by the vegetation canopy (FPAR) can be evaluated as

$$\begin{aligned}\mathrm{FPAR}(bio,p) &= \int_{400\mathrm{nm}}^{700\mathrm{nm}} \mathbf{a}_\lambda^{\mathrm{hem}}(\Omega_0)e(\lambda)\,d\lambda \\ &= Q_{bs}(bio,LAI,\Omega_0)+Q^q(bio,p,\Omega_0), \qquad (59)\end{aligned}$$

where

$$Q_{\mathrm{bs}}(bio,LAI,\Omega_0) = \int_{400\mathrm{nm}}^{700\mathrm{nm}} \mathbf{a}_{bs,\lambda}^{\mathrm{hem}}(\Omega_0)e(\lambda)\,d\lambda, \qquad (60)$$

$$\begin{aligned}Q^q(bio,p,\Omega_0) &= \int_{400\mathrm{nm}}^{700\mathrm{nm}} \mathbf{a}_{q,\lambda}(\Omega_0)\frac{\rho_{q,\mathrm{eff}}(\lambda)}{1-\rho_{q,\mathrm{eff}}(\lambda)\mathbf{r}_{q,\lambda}}\mathbf{t}_{\mathrm{bs},\lambda}^{\mathrm{hem},q}e(\lambda)\,d\lambda \qquad (61)\\ &= \int_{400\mathrm{nm}}^{700\mathrm{nm}} \frac{\mathbf{a}_{q,\lambda}(\Omega_0)}{\mathbf{t}_{q,\lambda}(\Omega_0)}\left[\tilde{A}_\lambda^{\mathrm{hem}}(\Omega_0)-\mathbf{r}_{\mathrm{bs},\lambda}^{\mathrm{hem}}(\Omega_0)\right]e(\lambda)\,d\lambda. \qquad (62)\end{aligned}$$

The Q_{bs} term describes the absorption within the canopy for a black-soil condition, and Q^q term describes the additional absorption within the canopy due to the interaction between the ground (soil and/or understory) and the canopy. Here $p\in P_{bio}$; e is the ratio of the monochromatic flux incident at the top surface of the canopy boundary to the total downward PAR flux which can be expressed as

$$e(\lambda)=\frac{E_{0,\lambda}e_\lambda^{\mathrm{hem}}(\Omega_0)}{\int_{400\mathrm{nm}}^{700\mathrm{nm}} E_{0,\lambda}e_\lambda^{\mathrm{hem}}(\Omega_0)\,d\lambda},$$

where $E_{0,\lambda}$ is the solar irradiance spectrum that is known for all wavelengths; e_λ^{hem} is the normalized incident irradiance defined as the ratio of the radiant incident on the surface to $E_{0,\lambda}$ [*Diner et al.*, 1998a]. The mean over those $p\in P_{bio}$ which passed the test $\Delta(p)\le h$ is taken as the estimate of FPAR, i.e.,

$$\mathrm{FPAR}_{bio}=\frac{1}{N_P}\sum_{k=1}^{N_P}\mathrm{FPAR}(bio,p),$$

where N_P is the number of canopy realizations $p\in P_{bio}$ passing this test. When there is no solution (i.e., F_{bio}=0), the algorithm defaults to a NDVI-FPAR regression analysis to obtain an estimate of FPAR [*Myneni et al*, 1997b].

The normalized incident irradiance and the BHR are provided by the MISR instrument at three spectral bands within the PAR region. We assume a piece-wise linear variation in these variables over regions [446, 558 nm], [558, 672 nm], and a constant over regions [400, 446 nm], [672, 700 nm]. Substituting these piece-wise linear functions into (59) and (62), one can express FPAR as a function of e_λ^{hem} and $\tilde{A}^{\mathrm{hem}}{}_\lambda$ [*Diner et al.*, 1998a]. Note that the dependence of FPAR on ground reflection properties is included in $\tilde{A}^{\mathrm{hem}}{}_\lambda$ which is provided by the MISR instrument; that is, expression (59) is a function of the biome type, Sun position, ground cover, mean leaf area index of an individual plant, and retrieved BHR.

If only MODIS observations are available for a given pixel or the MODIS-only mode is executed, $e(\lambda)$ is approximated by

$$e(\lambda)=\frac{E_\lambda(5200^0K)}{\int_{400\mathrm{nm}}^{700\mathrm{nm}} E_\lambda(5200^0K)},$$

where $E_\lambda(T)$ is the Planck function [*Kondratyev*, 1969, p. 230]. In this case, the Q^q term is a function of the biome type, Sun position, ground cover, mean leaf area index of an individual plant, and pattern of the effective ground reflectance. Expression (61) is used to evaluate this term. The Q_{bs} and Q^q terms are precomputed and stored in the look-up table.

9. Theoretical Basis of NDVI-FPAR Relations

The measured spectral reflectance data are usually compressed into vegetation indexes. More than a dozen such indexes are reported in the literature and shown to correlate well with vegetation amount [*Tucker*, 1979], the fraction of absorbed photosynthetically active radiation [*Asrar et al.*, 1984], unstressed vegetation conductance and photosynthetic capacity [*Sellers et al.*, 1992], and seasonal atmospheric carbon dioxide variations [*Tucker et al.*, 1986]. There are some theoretical investigations to explain these empirical regularities [*Vygodskaya and Gorshkova*, 1987; *Myneni et al.*, 1995a; *Verstraete and Pinty*, 1996]. Results from the previous section allow us to relate the vegetation indexes to the fundamental physical principle, i.e., the law of energy conservation. Here we consider the normalized difference vegetation index (NDVI) whose use is included in the LAI/FPAR retrieval algorithm.

Let us consider NDVI defined as

$$\mathrm{NDVI}=\frac{A_\alpha^{\mathrm{hem}}-A_\beta^{\mathrm{hem}}}{A_\alpha^{\mathrm{hem}}+A_\beta^{\mathrm{hem}}}, \tag{63}$$

where A_λ^{hem} is the BHR or DHR, and α and β are near-IR and red spectral wavebands, respectively. These variables are a function of Sun position Ω_0, but this dependence has been suppressed in the notation of this section. For the sake of simplicity, we consider the NDVI for the "black-soil" problem and "S problem." It follows from equations (48), (47), and (46) that equation (63) can be rewritten as

$$\mathrm{NDVI}=\frac{k(\alpha,\beta)\mathbf{a}(\beta)-m(\alpha,\beta)\mathbf{t}(\beta)}{2\mathbf{r}(\beta)+k(\alpha,\beta)\mathbf{a}(\beta)-m(\alpha,\beta)\mathbf{t}(\beta)}, \tag{64}$$

where

$$k(\alpha,\beta)=1-\frac{1-\gamma_{0,\mathbf{a}}(\beta)}{1-\gamma_{0,\mathbf{a}}(\alpha)}\cdot\frac{1-\omega(\alpha)}{1-\omega(\beta)},$$

$$m(\alpha,\beta)=\frac{1-\gamma_{0,\mathbf{t}}(\beta)}{1-\gamma_{0,\mathbf{t}}(\alpha)}-1.$$

Here $\gamma_{0,\mathbf{a}}$ and $\gamma_{0,\mathbf{t}}$ are defined by equation (49) with $K=K_{\mathbf{a}}$ (for canopy absorptance) and $K=K_{\mathbf{t}}$ (for canopy transmittance), respectively. Here the ratio between the leaf spectral reflectance and the leaf albedo is assumed to be constant with respect to wavelength, and so it is excluded from the argument list of $\mathbf{t}$. After simple transformations, one obtains

$$\mathrm{NDVI}=\mathbf{a}(\beta)\cdot\theta\left(s_{\mathbf{t},\beta},s_{\mathbf{r},\beta}\right),$$

where the function θ has the following form

$$s(x,y)=\frac{k(\alpha,\beta)-m(\alpha,\beta)\cdot x}{2y+k(\alpha,\beta)-m(\alpha,\beta)\cdot x},$$

$$s_{\mathbf{t},\beta}=\frac{\mathbf{t}(\beta)}{\mathbf{a}(\beta)},\qquad s_{\mathbf{r},\beta}=\frac{\mathbf{r}(\beta)}{\mathbf{a}(\beta)}.$$

Thus NDVI is proportional to the canopy absorptance at the red band. It follows from Eqs. (46) and (64) that

$$\mathbf{a}(\lambda)=\frac{1-\gamma_{0,\mathbf{a}}(\beta)}{1-\gamma_{0,\mathbf{a}}(\lambda)}\frac{1-\omega(\lambda)}{1-\omega(\beta)}\mathbf{a}(\beta)$$
$$=\frac{1-\gamma_{0,\mathbf{a}}(\beta)}{1-\gamma_{0,\mathbf{a}}(\lambda)}\frac{1-\omega(\lambda)}{1-\omega(\beta)}\frac{NDVI}{\theta(s_{\mathbf{t},\beta},s_{\mathbf{r},\beta})}.$$

Let $e(\lambda)$ be the ratio of monochromatic radiant energy incident on the top surface of the canopy boundary to the total PAR flux. Integrating $e\cdot\mathbf{a}$ over the PAR region of solar spectrum, we get

$$\mathrm{FPAR}=k\cdot\mathrm{NDVI},$$

where

$$k=\frac{1}{\theta\left(s_{\mathbf{t},\beta},s_{\mathbf{r},\beta}\right)}\frac{1-\gamma_{0,\mathbf{a}}(\beta)}{1-\omega(\beta)}\left[\int_{400}^{700}\frac{1-\omega(\lambda)}{1-\gamma_{0,\mathbf{a}}(\lambda)}e(\lambda)\,d\lambda\right].$$

Thus if the canopy ground is ideally black, FPAR is proportional to NDVI. The factor of proportionality k depends on the ratios $s_{\mathbf{t},\beta}$ and $s_{\mathbf{t},\beta}$, the coefficients $K_{\mathbf{a}}$ and $K_{\mathbf{t}}$, and the leaf albedo at the red and near-IR spectral bands. A relationship between NDVI and FPAR which accounts for the soil contribution can be derived from equation (27) in a similar manner. Other types of vegetation indexes can be derived in an analogous way.

10. Concluding Remarks

This paper presents the theoretical basis of the algorithm designed for the retrieval of LAI and FPAR synergistically from MODIS and MISR data. A three-dimensional formulation of the radiative transfer process is used to derive simple but correct relationships between spectral and angular biome-specific signatures of vegetation canopies and the structural and optical characteristics of the vegetation canopies. However, these relationships are not directly used to obtain the best fit with measured spectral and angular canopy reflectances. Accounting for features specific to the problem of radiative transfer in plant canopies, we adopt powerful techniques developed in nuclear reactor theory and atmospheric physics in the retrieval algorithm. This technique allows us to explicitly separate the contribution of soil/understory reflectance to the exitant radiation field, to relate hemispherically integrated reflectances to optical properties of phytoelements and to split the complicated radiative transfer problem into several independent simpler subproblems, the solutions of which are precomputed and stored in a form of look-up table, and then used to retrieve LAI and FPAR. The solutions of the subproblems are components of various forms of energy conservation principle (e.g., canopy transmittance and absorptance of a vegetation canopy bounded by vacuum on all sides). They are determined from general properties of radiative transfer and are independent of the models used to generate the LUT. Thus we express the angular and spectral signatures of vegetation canopies in terms of the energy conservation principle. It allows the design of an algorithm that returns values of LAI and FPAR which provide the best agreement not only to measured data but which also conform to the energy conservation law. Since the algorithm interacts only with the elements of the LUT, its functioning does not depend on any particular canopy radiation model. This flexible feature allows the use of the best canopy radiation models for the generation of the LUT.

Appendix

A rather wide family of canopy radiation models include the following steps in their formulation:

1. The attenuation of direct and diffuse incident radiation $L_{\lambda,0}$ is evaluated. It satisfies the equation

$$\Omega\bullet\nabla L_{\lambda,0}(r,\Omega)+\sigma(r,\Omega)L_{\lambda,0}(r,\Omega)=0 \tag{A1}$$

and boundary conditions (14)-(16). The solution of this boundary value problem can be explicitly expressed in many

practical cases. Here σ is the total interaction cross section defined as

$$\sigma(r,\Omega) = G(r,\Omega)\langle u_L(r)\rangle_{\text{bio}} . \quad \text{(A2)}$$

2. The upward once-scattered radiation $L_{\lambda,1}$ is evaluated. It satisfies the equation

$$\Omega \bullet \nabla L_{\lambda,1}(r,\Omega) + \sigma_1(r,\Omega)L_{\lambda,1}(r,\Omega) = \frac{\langle u_L(r)\rangle_{\text{bio}}}{\pi}\int_{4\pi}\Gamma_\lambda(r,\Omega'\to\Omega)L_{\lambda,0}(r,\Omega')\,d\Omega' \quad \text{(A3)}$$

and the vacuum boundary condition; that is,

$$L_{\lambda,1}(r,\Omega) = 0, \qquad r\in\delta V, \qquad \Omega\bullet \mathrm{n}_r < 0,$$

where n_r is the outward normal at point $r\in\delta V$. The total interaction cross-section σ_1 is defined as

$$\sigma_1(r,\Omega) = p(r,\Omega,\Omega_0)G(r,\Omega)\langle u_L(r)\rangle_{\text{bio}}, \quad \text{(A4)}$$

where p is the bidirectional gap probability (section 2). This boundary value problem allows for an explicit solution in many practical situations.

3. The multiply scattered radiance is evaluated by solving the transport equation

$$\Omega \bullet \nabla L_{\lambda,M}(r,\Omega) + \sigma(r,\Omega)L_{\lambda,M}(r,\Omega) = \frac{\langle u_L(r)\rangle_{\text{bio}}}{\pi}\int_{4\pi}\Gamma_\lambda(r,\Omega'\to\Omega)\left[L_{\lambda,M}(r,\Omega') + L_{\lambda,1}(r,\Omega')\right]d\Omega' \quad \text{(A5)}$$

with the boundary conditions expressed by

$$L_{\lambda,M}(r_t,\Omega) = 0, \qquad \Omega\bullet \mathrm{n}_t < 0,$$

$$L_{\lambda,M}(r_1,\Omega) = \frac{1}{\pi}\int_{\Omega'\bullet \mathrm{n}_l>0} R_{l,\lambda}(\Omega',\Omega)L_{\lambda,M}(r_1,\Omega')|\Omega'\bullet \mathrm{n}_l|\,d\Omega' + \frac{1}{\pi}\int_{\Omega'\bullet \mathrm{n}_l>0} R_{l,\lambda}(\Omega',\Omega)L_{\lambda,1}(r_1,\Omega')|\Omega'\bullet \mathrm{n}_l|\,d\Omega',$$

$$r_1\in\delta V_1, \Omega\bullet \mathrm{n}_1 < 0,$$

$$L_{\lambda,M}(r_b,\Omega) = \frac{1}{\pi}\int_{\Omega'\bullet \mathrm{n}_b>0} R_{b,\lambda}(\Omega',\Omega)L_{\lambda,M}(r_b,\Omega')|\Omega'\bullet \mathrm{n}_b|\,d\Omega' + \frac{1}{\pi}\int_{\Omega'\bullet \mathrm{n}_b>0} R_{b,\lambda}(\Omega',\Omega)L_{\lambda,1}(r_b,\Omega')|\Omega'\bullet \mathrm{n}_b|\,d\Omega',$$

$$r_b\in\delta V_b, \Omega\bullet \mathrm{n}_b < 0.$$

The monochromatic radiance is given in such models as

$$L_\lambda(r,\Omega) = L_{\lambda,0}(r,\Omega) + L_{\lambda,1}(r,\Omega) + L_{\lambda,M}(r,\Omega). \quad \text{(A6)}$$

There may be some differences in formulations of the subproblems 1, 2, and 3. However, all such models have one property in common: the original total interaction cross-section (A2) is replaced by another coefficient (A4) when one evaluates the distribution of the single-scattered radiation field. This trick allows the inclusion of the hot spot effect into canopy radiation models.

Equation (A3) can be rewritten in an equivalent form as

$$\Omega \bullet \nabla L_{\lambda,1}(r,\Omega) + \sigma(r,\Omega)L_{\lambda,1}(r,\Omega) = \frac{\langle u_L(r)\rangle_{\text{bio}}}{\pi}\int_{4\pi}\Gamma_\lambda(r,\Omega'\to\Omega)L_{\lambda,0}(r,\Omega')\,d\Omega' + \left[\sigma(r,\Omega) - \sigma_1(r,\Omega)\right]L_{\lambda,1}, \quad \text{(A7)}$$

It follows from summarizing Eqs. (A1), (A5), and (A7) that the radiance (A6) satisfies equation (13) with F defined as

$$F_\lambda(r,\Omega) = \left[\sigma(r,\Omega) - \sigma_1(r,\Omega)\right]L_{\lambda,1},$$

and boundary conditions expressed by Eqs. (14)-(16). Thus such models describe radiation regime in a vegetation canopy generated by incoming radiation and an internal source F_λ. This source appears due to the changes in the extinction coefficient when one tries to account for the hot spot effect.

Acknowledgments. This research was carried out by Department of Geography, Boston University, under contract with the National Aeronautics and Space Administration.

References

Anisimov, O. A., and G. V. Menzulin, The problem of modeling the radiative radiation regime in the plant cover, *Sov. Meteorol. and Hydrol., 10*, 70-74, 1981.

Asrar, G., M. Fuchs, E.T. Kanemasu, and J.L.Hatfield, Estimating absorbed photosynthetic radiation and leaf area index from spectral reflectance in wheat, *Agron. J., 76*, 300-306, 1984.

Baret, F., S. Jacquemoud, and J.F. Hanocq, The soil concept in remote sensing, *Remote Sens. Rev., 7*, 65-82, 1993.

Borel, C.C., S.A., Gerstl, and B.J. Powers, The radiosity method in optical remote sensing of structured 3-D surfaces, *Remote Sens. Environ., 36*, 13-44, 1991.

Deschamps, P.Y., F.M. Bréon, M. Leroy, A. Podaire, A. Bricaud, J.C. Buriez, and G. Sèze, The POLDER mission: Instrument characteristics and scientific objectives, *IEEE Trans. Geosci. Remote Sens., GE-32*, 598-615, 1994.

Diner, D.J., J.V.Martonchik, C. Borel, S.A.W. Gerstl, H.R. Gordon, Y. Knyazikhin, R. Myneni, B. Pinty, and M.M. Verstraete, MISR: Level 2 surface retrieval algorithm theoretical basis, *JPL Internal Doc. D-11401, Rev. C*, Calif. Inst. of Technol., Jet Propul. Lab., Pasadena, 1998a.

Diner, D.J., W.A. Abdou, H.R. Gordon, R.A. Kahn, Y. Knyazikhin, J.V.Martonchik, S. McMuldroch, R.B. Myneni, and R.A. West, Level 2 ancillary products and data sets algorithm theoretical basis, *JPL Internal Doc. D-13402, Rev. A*, Calif. Inst. of Technol., Jet Propul. Lab., Pasadena, 1998b.

Germogenova, T.A., *The Local Properties of the Solution of the Transport Equation* (in Russian), 272 pp., Nauka, Moscow, 1986.

Jacquemoud, S., F. Barret, and J.F. Hanocq, Modeling spectral and bidirectional soil reflectance, *Remote Sens. Environ., 41*, 123-132, 1992.

Kimes, D.S., Radiative transfer in homogeneous and heterogeneous vegetation canopies, in *Photon-Vegetation Interactions: Applications in Plant Physiology and Optical Remote Sensing*, pp. 339-388, edited by R. B. Myneni and J. Ross, Springer-Verlag, New York, 1991.

Knyazikhin, Y., and A. Marshak, Fundamental equations of radiative transfer in leaf canopies and iterative methods for their solution, in *Photon-Vegetation Interactions: Applications in Plant Physiology and Optical Remote Sensing*, pp. 9-43, edited by R. B. Myneni and J. Ross, Springer-Verlag, New York, 1991.

Knyazikhin, Y., J. Kranigk, G. Miessen, O. Panfyorov, N. Vygodskaya, and G. Gravenhorst, Modelling three-dimensional

distribution of photosynthetically active radiation in sloping coniferous stands, *Biomass Bioenerg., 2/3*, 189-200, 1996.

Knyazikhin, Y., J. Kranigk, R.B. Myneni, O.Panfyorov, and G.Gravenhorst, Influence of small-scale structure on radiative transfer and photosynthesis in vegetation cover, *J. Geophys. Res., 103*, 6133-6144, 1998.

Knyazikhin, Y., J.V. Martonchik, D.J.Diner, R.B. Myneni, M.M. Verstraete, B.Pinty, and N. Gobron, Estimation of vegetation canopy leaf area index and fraction of absorbed photosynthetically active radiation from atmosphere-corrected MISR data, this issue.

Kondratyev, K. Y., *Radiation in the Atmosphere*, 912 pp., Academic, San Diego, Calif., 1969.

Krein, S.G (Ed.), *Functional Analysis*, 352 pp., Foreign Technol. Div., Wright-Patterson Air Force Base, Ohio, 1967.

Kuusk, A., The hot-spot effect of a uniform vegetative cover, *Sov. J. Remote. Sens, 3*, 645-658, 1985.

Li, X., and A. Strahler, Geometric-optical modeling of a coniferous forest canopy, *IEEE Trans. Geosci. Remote Sens., GE-23*, 207-221, 1985.

Li, X., A. Strahler, and C. E. Woodcock, A hybrid geometric optical-radiative transfer approach for modelling albedo and directional reflectance of discontinuous canopies, *IEEE Trans. Geosci. Remote Sens., 2*, 466-480, 1995.

Liou, K.-N., *An Introduction to Atmospheric Radiation*, 392 pp., Academic, San Diego, Calif., 1980.

Marshak, A., Effect of the hot spot on the transport equation in plant canopies, *J. Quant. Spectrosc. Radiat. Transfer, 42,* 615-630, 1989.

Martonchik, J.V., D.J.Diner, B.Pinty, M.M.Verstraete, R.B.Myneni, Y.Knyazikhin, and H.R.Gordon, Determination of land and ocean reflective, radiative and biophysical properties using multi-angle imaging, *IEEE Trans. Geosci. Remote Sens., 36*, 1266-1281, 1998.

Myneni, R.B., Modeling radiative transfer and photosynthesis in three-dimensional vegetation canopies, *Agric. For. Meteorol., 55*, 323-344, 1991.

Myneni, R. B., and G. Asrar, Photon interaction cross sections for aggregations of finite dimensional leaves, *Remote Sens. Environ., 37*, 219-224, 1991.

Myneni, R. B., and D. L. Williams, On the relationship between FAPAR and NDVI, *Remote Sens. Environ., 49*, 200-211, 1994.

Myneni, R.B., J. Ross, and G. Asrar, A review on the theory of photon transport in leaf canopies in slab geometry, *Agric. For. Meteorol., 45*, 1-165, 1989.

Myneni, R.B., A.L. Marshak, and Y. V. Knyazikhin, Transport theory for a leaf canopy of finite-dimensional scattering centers, *Quant. Spectrosc. Radiat. Transfer, 46*, 259-280, 1991.

Myneni, R.B., F.G. Hall, P.J. Sellers, and A.L. Marshak, The interpretation of spectral vegetation indexes, *IEEE Trans. Geosci. Remote Sens., 33*, 481-486, 1995a.

Myneni,R.B., S. Maggion, J. Iaquinta, J.L. Privette, N. Gobron, B. Pinty, D.S. Kimes, M.M. Verstraete, and D.L. Williams, Optical remote sensing of vegetation: Modeling, caveats and algorithm, *Remote Sens. Environ, 51*, 169-188, 1995b.

Myneni,R.B., C.D. Keeling, C.J. Tucker, G.Asrar, and R.R. Nemani, Increased plant growth in the northern high latitudes from 1981 to 1991, *Nature, 386*, 698-702, 1997a.

Myneni, R.B., R.R. Nemani, and S.W. Running, Estimation of global leaf area index and absorbed PAR using radiative transfer model, *IEEE Trans. Geosci. Remote Sens., 35*, 1380-1393, 1997b.

Nilson, T., A theory of radiation penetration into non-homogeneous plant canopies, in *The Penetration of Solar Radiation into Plant Canopies* (in Russian), pp. 5-70, Estonian Acad. of Sci., Tartu, 1977.

Norman, J.M., and J. M. Welles, Radiative transfer in an array of canopies, *Agron. J., 75*, 481-488, 1983.

Oker-Blom, P., J. Lappi., and H. Smolander, Radiation regime and photosynthesis of coniferous stands, in *Photon-Vegetation Interactions: Applications in Plant Physiology and Optical Remote Sensing*, pp. 469-499, edited by R. B. Myneni and J. Ross, Springer-Verlag, New York, 1991.

Privette, J. L., R. B. Myneni, W. L. Emery, and C. J. Tucker, Invertibility of a 1D discrete ordinates canopy reflectance model, *Remote Sens. Environ., 48*, 89-105, 1994.

Ross, J., *The Radiation Regime and Architecture of Plant Stands*, 391 pp., Dr. W. Junk, Norwell, Mass., 1981.

Ross, J.K., and A. L. Marshak, Calculation of the solar radiation reflection from plant cover using the Monte-Carlo method, *Sov. J. Remote. Sens., 5*, 58-67, 1984.

Ross, J., and T. Nilson, The calculation of photosynthetically active radiation in plant communities, in *Solar Radiation Regime in Plant Stand* (in Russian), pp. 5-54, Estonian Acad of Sci. Inst. Phys. Astron., Tartu, 1968.

Ross, J., Y. Knyazikhin, A. Kuusk, A. Marshak, and T. Nilson, *Mathematical Modeling of the Solar Radiation Transfer in Plant Canopies* (in Russian, with English abstract), 195 pp., Gidrometeoizdat, St. Peterburg, Russia, 1992.

Sellers, P.J., J.A. Berry, G.J. Gollatz, C.B.Field, and F.G. Hall, Canopy reflectance, photosynthesis and transpiration, III, A reanalysis using improved leaf models and a new canopy integration scheme, *Remote Sens. Environ., 42*, 187-216, 1992.

Sellers, P.J., et al., Modeling the exchange of energy, water, and carbon between continents and atmosphere, *Science, 275*, 602-509, 1997.

Simmer, C., and S.A. Gerstl, Remote sensing of angular characteristics of canopy reflectances, *IEEE Trans. Geosci. Remote Sens., GE-23*, 648-658, 1985.

Titov, G.A., Statistical description of radiative transfer in clouds, *J. Atmos. Sci.,47*, 24-38, 1990.

Tucker, C.J., Red and photographic infrared linear combination for monitoring vegetation, *Remote Sens. Environ., 8*, 127-150, 1979.

Tucker, C.J., Y.Fung, C.D. Keeling, and R.H. Gammon, Relationship between atmospheric CO_2 variations and a satellite-derived vegetation index, *Nature, 319*, 195-199, 1986.

Vainikko, G.M, Equation for mean intensity in broken clouds (In Russian), *Meteorol. Issled., 21*, 28-37, 1973.

Vermote, E., L. A. Remer, C. O. Justice, Y. J. Kaufman, and D. Tanré, Atmospheric correction algorithm: Spectral reflectances (MOD09), version 2.0, Algorithm technical background document, *NASA EOS-ID 2015 Doc.*, 42 pp., 1995.

Verstraete, M.M., and B. Pinty, Designing spectral indexes for remote sensing applications, *IEEE Trans. Geosci. Remote Sens., 34*, 1254-1265, 1996.

Verstraete M.M., B. Pinty, and R.E. Dickenson, A physical model of the bidirectional reflectance of vegetation canopies, *J. Geophys. Res., 95*, 11765-11775, 1990.

Vladimirov, V.S., Mathematical problems in the one-velocity theory of particle transport, *Tech. Rep. AECL-1661*, At. Energy of Can. Ltd., Chalk River, Ontario, 1963.

Vygodskaya, N.N., and I.I. Gorshkova, *Theory and Experiment in Vegetation Remote Sensing* (in Russian, with English abstract), 248 pp., Gidrometeoizdat, St. Petesburg, Russia, 1987.

D.J. Diner, and J.V. Martonchick, Mail Stop 169-237, Jet Propulsion Laboratory, California Institute of Technology, 4800 Oak Grove Drive, Pasadena, CA-91109. (e-mail: djd@jord.jpl.nasa.gov; jvm@ jord.jpl.nasa.gov)

Y. Knyazikhin, and R. B. Myneni, Department of Geography, Boston University, 675 Commonwealth Avenue, Boston, MA 022150. (e-mail: jknjazi@crsa.bu.edu; rmyneni@crsa.bu.edu)

S. W. Running, The School of Forestry, University of Montana, Missoula, MT 59812. (e-mail: swr@ntsg.umt.edu)

(Received January 8, 1998; revised May 1, 1998;
accepted July 22, 1998.)